



OPEN ACCESS

EDITED BY

Valentin P. Yakubenko,
East Tennessee State University,
United States

REVIEWED BY

Liwu Li,
Virginia Tech, United States
Francesca Odoardi,
Medical University Göttingen, Germany
Naoto Kawakami,
Ludwig Maximilian University of Munich,
Germany

*CORRESPONDENCE

Barbara Rossi

✉ barbara.rossi@univr.it

Gabriela Constantin

✉ gabriela.constantin@univr.it

SPECIALTY SECTION

This article was submitted to
Molecular Innate Immunity,
a section of the journal
Frontiers in Immunology

RECEIVED 16 October 2022

ACCEPTED 05 April 2023

PUBLISHED 18 April 2023

CITATION

Rossi B, Dusi S, Angelini G, Bani A,
Lopez N, Della Bianca V, Pietronigro EC,
Zenaro E, Zocco C and Constantin G
(2023) Alpha4 beta7 integrin controls Th17
cell trafficking in the spinal cord
leptomeninges during experimental
autoimmune encephalomyelitis.
Front. Immunol. 14:1071553.
doi: 10.3389/fimmu.2023.1071553

COPYRIGHT

© 2023 Rossi, Dusi, Angelini, Bani, Lopez,
Della Bianca, Pietronigro, Zenaro, Zocco and
Constantin. This is an open-access article
distributed under the terms of the [Creative
Commons Attribution License \(CC BY\)](https://creativecommons.org/licenses/by/4.0/). The
use, distribution or reproduction in other
forums is permitted, provided the original
author(s) and the copyright owner(s) are
credited and that the original publication in
this journal is cited, in accordance with
accepted academic practice. No use,
distribution or reproduction is permitted
which does not comply with these terms.

Alpha4 beta7 integrin controls Th17 cell trafficking in the spinal cord leptomeninges during experimental autoimmune encephalomyelitis

Barbara Rossi^{1*}, Silvia Dusi¹, Gabriele Angelini¹,
Alessandro Bani¹, Nicola Lopez¹, Vittorina Della Bianca¹,
Enrica Caterina Pietronigro¹, Elena Zenaro¹, Carlotta Zocco¹
and Gabriela Constantin^{1,2*}

¹Department of Medicine, University of Verona, Verona, Italy, ²The Center for Biomedical Computing (CBMC), University of Verona, Verona, Italy

Th1 and Th17 cell migration into the central nervous system (CNS) is a fundamental process in the pathogenesis of experimental autoimmune encephalomyelitis (EAE), the animal model of multiple sclerosis (MS). Particularly, leptomeningeal vessels of the subarachnoid space (SAS) constitute a central route for T cell entry into the CNS during EAE. Once migrated into the SAS, T cells show an active motility behavior, which is a prerequisite for cell-cell communication, *in situ* reactivation and neuroinflammation. However, the molecular mechanisms selectively controlling Th1 and Th17 cell trafficking in the inflamed leptomeninges are not well understood. By using epifluorescence intravital microscopy, we obtained results showing that myelin-specific Th1 and Th17 cells have different intravascular adhesion capacity depending on the disease phase, with Th17 cells being more adhesive at disease peak. Inhibition of α L β 2 integrin selectively blocked Th1 cell adhesion, but had no effect on Th17 rolling and arrest capacity during all disease phases, suggesting that distinct adhesion mechanisms control the migration of key T cell populations involved in EAE induction. Blockade of α 4 integrins affected myelin-specific Th1 cell rolling and arrest, but only selectively altered intravascular arrest of Th17 cells. Notably, selective α 4 β 7 integrin blockade inhibited Th17 cell arrest without interfering with intravascular Th1 cell adhesion, suggesting that α 4 β 7 integrin is predominantly involved in Th17 cell migration into the inflamed leptomeninges in EAE mice. Two-photon microscopy experiments showed that blockade of α 4 integrin chain or α 4 β 7 integrin selectively inhibited the locomotion of extravasated antigen-specific Th17 cells in the SAS, but had no effect on Th1 cell intratissue dynamics, further pointing to α 4 β 7 integrin as key molecule in Th17 cell trafficking during EAE development. Finally, therapeutic inhibition of α 4 β 7 integrin at disease onset by intrathecal injection of a blocking antibody attenuated clinical severity and reduced neuroinflammation, further demonstrating a crucial role for α 4 β 7 integrin in driving Th17 cell-mediated

disease pathogenesis. Altogether, our data suggest that a better knowledge of the molecular mechanisms controlling myelin-specific Th1 and Th17 cell trafficking during EAE development may help to identify new therapeutic strategies for CNS inflammatory and demyelinating diseases.

KEYWORDS

alpha4 beta7 integrin, Th1 cells, Th17 cells, leptomeninges, intravital microscopy, experimental autoimmune encephalomyelitis

Introduction

T cells constantly circulate in the bloodstream searching for the right signals to migrate into lymphoid or non-lymphoid organs. Several steps are required for T cells to arrive in a target site. Firstly, they need to cross the vascular wall of the post-capillary venules, a process that is governed by a sequence of events including: 1) tethering and rolling, which are mediated by the interactions between selectins and mucins, and/or between integrins and adhesion molecules from the immunoglobulin superfamily; 2) activation induced by chemoattractants, leading to integrin activation; 3) arrest and intravascular crawling mediated by integrins and their endothelial ligands; and 4) diapedesis or transmigration, which represents a complex step mediated by receptors such as endothelial cadherins and junctional adhesion molecules (1, 2). After extravasation, T cells may perform long-spread migration and communicate with other cells by chemical signaling and cell-cell physical interactions. The dynamic behavior of T cells is crucial for antigen recognition, proliferation and survival, leading to immune response development (3, 4). Indeed, *in vivo* high motility capability of T cells is an essential feature for an efficient antigen scanning in lymphoid organs or inflamed target tissues (5–7).

Multiple sclerosis (MS) and its animal model, experimental autoimmune encephalomyelitis (EAE), are considered autoimmune diseases mediated by myelin-specific encephalitogenic T lymphocytes, which migrate into the central nervous system (CNS) and become reactivated by local antigen presenting cells (APCs) (8, 9). Using a transfer model of EAE and two-photon laser scanning microscopy (TPLSM), previous studies demonstrated that pioneer T cells preferentially enter the CNS migrating across pial vessels within the meningeal space. Here, T cells assume a “migratory phenotype” leading to the subsequent invasion of spinal cord parenchyma, which represents a fundamental step for clinical EAE development (10). In addition, epifluorescence intravital microscopy (EIVM) studies performed by our laboratory demonstrated that activated T cell adhesion in inflamed CNS pial vessels is controlled by commonly used leukocyte adhesion molecules, such as selectins, mucins, chemokines, integrins and members of the immunoglobulin superfamily (11–16). Currently, it is well established that $\alpha 4$ integrins are key players in mediating tethering and rolling as well as firm adhesion of encephalitogenic T cells in inflamed

brain pial venules (14). However, the individual contributions of the two related $\alpha 4$ integrins, $\alpha 4\beta 1$ (or very late antigen-4 (VLA-4)) and $\alpha 4\beta 7$ (also known as lymphocyte Peyer’s patch adhesion molecule (LPAM)), in intravascular T cell rolling and firm adhesion (arrest) during EAE is not well understood. Also, how adhesion molecules control the motility behavior of infiltrating encephalitogenic T cells inside the subarachnoid space (SAS) during early EAE and the subsequent penetration of T cells into the CNS parenchyma were not well investigated.

A role for lymphocyte function-associated antigen-1 (LFA-1 or $\alpha L\beta 2$) in the amoeboid encephalitogenic T cell migration in the SAS during EAE was recently established, but whether $\alpha 4$ integrins also contribute to T cell motility behavior is unclear (17). In this work, we investigated the roles of $\alpha 4$ integrins in the migration of Th1 and Th17 cells, two cell populations involved in the induction of autoimmunity and neuroinflammation during EAE (18). We first studied the roles of $\alpha 4\beta 1$ and $\alpha 4\beta 7$ integrins in Th1 and Th17 cell intravascular adhesion by using EIVM in the spinal cord leptomeningeal venules at different disease phases in mice immunized with the myelin oligodendrocyte glycoprotein (MOG)₃₅₋₅₅ peptide. Then, we performed TPLSM studies to determine the role of $\alpha 4$ integrins in the spinal cord SAS motility behavior of adoptively transferred Th1 and Th17 cells. Our data show that, whereas VLA-4 has a central role in Th1 cell migration, $\alpha 4\beta 7$ integrin is selectively involved in Th17 cell trafficking in the leptomeninges during EAE, suggesting that understanding integrin-dependent T cell dynamics may lead to the therapeutic modulation of immune responses during CNS inflammatory and autoimmune diseases (19).

Materials and methods

Study approval

The studies involving mice were authorized by the Italian Ministry of Health, Department of Veterinary Public Health, Nutrition and Food Safety, Directorate General of Animal Health and Veterinary Medicine, as required by the Italian legislation (D.Lgs 26/2014, application of European Directive 2010/63/EU). Protocol numbers 33588, 30969 and 96/2023-PR were used for the *in vivo* studies in this manuscript.

Mice

C57BL/6J wild-type (WT) mice and C57BL/6-Tg (Tcra2D2, Tcrb2D2)1Kuch/J (2D2 TCR) transgenic mice carrying a T cell receptor specific for the MOG₃₅₋₅₅ peptide (20) were obtained from The Jackson Laboratory. All efforts were made to minimize the number of animals used and their suffering during the experimental procedure. All animal experiments were supervised by the local Institutional Animal Care Committee (OPBA) of the University of Verona and were conducted according to current European Community rules and approved protocols as mentioned above.

Production of MOG₃₅₋₅₅-specific Th1 and Th17 cells

Spleens were collected from 2D2 TCR transgenic mice, and a single-cell suspension was prepared and cultured as previously described (17). Briefly, splenocytes were cultured in the presence of 20 µg/ml MOG₃₅₋₅₅ peptide (GenScript Corporation). Th1 polarization was induced by *in vitro* stimulation with 1 ng/ml IL-12 (R&D Systems) and 10 µg/ml anti-IL-4 antibody (clone 11B11, hybridoma kindly provided by E. C. Butcher, Stanford University), while Th17 polarization was induced by using 5 ng/ml TGF-β, 20 ng/ml IL-6 and 2 ng/ml IL-23 (all from Miltenyi Biotec or R&D Systems), as well as 10 µg/ml anti-IL-4 antibody (as above) and 10 µg/ml anti-IFNγ antibody (clone HB170, R&D Systems). After 4 days in culture, Th1 and Th17 cells were supplemented with IL-2 (20 U/ml) or IL-7 (10 ng/ml) respectively for other 72 h. MOG₃₅₋₅₅-specific Th1 and Th17 cells were then isolated using a Ficoll-Paque density gradient (GE Healthcare Life Sciences) and re-stimulated for 3 days in the presence of irradiated splenocytes as APCs (APC:T cell ratio = 5:1) with the same protocol used for the first stimulation. Th1 and Th17 cells were then isolated as described above and supplemented for one further day with IL-2 or IL-7, respectively. Th1 and Th17 polarization was confirmed by flow cytometry (Supplementary Figures 1A, B) as previously described (17).

Isolation of Th1 and Th17 cells from EAE induced mice tissues

Endogenous leukocytes were collected from the blood and spinal cord of C57BL/6 MOG₃₅₋₅₅-immunized EAE mice at disease peak. Exogenous *in vitro* differentiated CMAC-labelled Th1 or Th17 cells were injected in EAE mice at disease onset and collected from the spinal cord 48 h later. Blood was harvested from retro-orbital plexus of anesthetized mice before perfusion, and leukocytes separated from red cells by dextran sedimentation followed by hypotonic lysis. Mice were then immediately perfused through the left cardiac ventricle by injecting cold phosphate buffered saline (PBS) supplemented with 1mM Ca²⁺/Mg²⁺. Spinal cords were collected, homogenized using GentleMACS Octo Dissociator (Miltenyi Biotec), enzymatically digested with 1 mg/ml collagenase (Sigma Aldrich) and 40 U/ml DNase (Thermo Fisher Scientific) for 45min at 37°C and leukocytes isolated from the

cell suspension by Percoll gradient centrifugation as previously described (17).

Flow cytometry

In vitro differentiated Th1 and Th17 cells were stimulated for 12 h with 50 ng/ml phorbol 12-myristate 13-acetate (PMA), 1µg/ml ionomycin, and 10µg/ml brefeldin A for cytokine production assessment. Cells were fixed and permeabilized and labelled with FITC-conjugated anti-IFNγ and PE-conjugated anti IL-17 antibodies (Biolegend). *In vitro* differentiated Th1 and Th17 cells were also stained with the following rat anti-mouse unconjugated monoclonal antibodies for the evaluation of adhesion molecule expression: anti-CD49d (clone PS-2), anti-LPAM-1 (clone DATK32), anti-CD44 (clone MJ64), anti- CD11a/CD18 (clone TIB213), anti-L-selectin (clone MEL-14) and anti-PSGL-1 (clone 2PH1). A PE Goat anti-rat IgG was used as secondary antibody (Biolegend). For *ex vivo* studies, in exogenous Th1 and Th17 cells, the mean fluorescence intensity (MFI) of α4β7 expression (FITC- conjugated anti-α4β7 antibody; BidScientific) was calculated on live CMAC+ infiltrating cells. Endogenous Th1 and Th17 cells were identified by chemokine receptors profile and assessed for α4β7 expression by using the following antibody panel: VioBlue-conjugated anti-CD45 (Miltenyi Biotec), VioGreen-conjugated anti-CD45 (Miltenyi Biotec), FITC- conjugated anti-α4β7 (BidScientific), PE-conjugated anti-CCR6 (Biolegend), PE-Cy7-conjugated anti-CXCR3 (Biolegend), APC-conjugated anti-CCR4 (Biolegend). Cell viability was assessed by 7-AAD labelling (Biolegend) for freshly isolated cells or by Viability 405/520 Fixable Dye (Miltenyi Biotec) for fixed cells. Cells were acquired by a MACSQuant Analyzer (Miltenyi Biotec) and the analysis was performed with FlowJo software.

Surgical procedures for intravital microscopy

Mice were anesthetized and prepared for surgery to expose the lumbar column over L1-L4 leaving an intact dura mater as previously described (17). Mice were positioned on the stabilizing device and maintained at 37°C. Local administration of few drops of artificial CSF on surgically exposed spinal cord (Cold Spring Harb Protoc; 2011; doi:10.1101/pdb.rec065730) allowed the direct immersion of the microscope objectives.

Epifluorescence intravital microscopy (EIVM)

Th1 and Th17 cells were labeled for 5 min at 37°C with either green 5-chloromethylfluorescein diacetate (CMFDA) or orange 5-(and-6)-(((chloromethyl)benzoyl)amino)tetramethylrhodamine (CMTMR) (both from Molecular Probes) (11). 3×10^7 of differentially labelled Th1 and Th17 cells were then intravenously injected immediately before imaging into MOG₃₅₋₅₅-immunized

EAE recipient mice at different disease phases. In some experiments, cells were preincubated with blocking antibodies and compared to untreated control T cells. Particularly, Th1 and Th17 cells were incubated with 100 µg/ml of anti- $\alpha 4$ integrins (clone PS/2, rat anti-mouse) or anti- $\alpha 4\beta 7$ integrin (clone DATK32, rat anti-mouse), anti-LFA-1 (clone TIB213, rat anti-mouse) for 5 min at 37°C and then injected with a supplement of up to 100 µg of blocking antibody (11). Mice were placed under a water immersion objective with a long focal distance (Olympus Achroplan, focal distance 3.3 mm, NA 0.5) of an upright Olympus BX50WI microscope. A Sony SSM-125CE monitor linked to a VE-1000 SIT analog monochromatic silicon-intensified target camera (Dage-MTI) allowed images visualization while an HDV DN-400 recorder (Datavideo Technologies Co.) was used for digitalization and storage of real-time movies (16) (Supplementary Movie 1).

EIVM data analysis

Manually analysis of digital video files was performed frame by frame at intervals of 0.04 s (25 frames) by ImageJ (National Institutes of Health). Venule diameters and cell velocities were measured for the hemodynamic parameters. Particularly, the velocities of 20 consecutive freely-flowing cells per vessel were manually measured for the determination of the fastest one. From the velocity of the fastest cell of each analyzed vessel (V_{max}), we calculated the mean blood flow velocities (V_m) according to equation: $V_m = V_{max}/(2 - \epsilon^2)$ where ϵ is the ratio of lymphocyte diameter to the vessel diameter and the critical velocity (V_{crit}), which was determined by using the following equation: $V_{crit} = V_m \times \epsilon \times (2 - \epsilon)$. Wall shear stress (WSS) was calculated as wall shear rate (WSR) multiplied by an assumed blood viscosity of 0.025 Poise where WSR is determined by the formula: $WSR = 8 \times V_m/\text{vessel diameter}$. At least 100 consecutive cells/venule were examined to determine the cell fraction that was rolling or performed arrest within a given vessel. A cell was considered as rolling if traveled at a velocity lower than the V_{crit} whereas the arrest was considered when a cell remained stationary on the venule wall for ≥ 30 seconds (11, 21, 22).

TPLSM imaging

Th1 or Th17 cells were labeled for 45 min at 37°C with 7-amino-4-chloromethylcoumarin (CMAC) (Molecular Probes). Then, 2×10^7 Th1 or Th17 cells were intravenously injected into MOG₃₅₋₅₅-immunized EAE recipient mice at the onset of the disease. After 48 h, when mice reached the EAE peak, 70 kDa fluorescein isothiocyanate dextran (FITC-dextran) (Sigma Chemical Co., St. Louis, MI, USA) was intravenously injected immediately before imaging of blood vessels. A mode-locked Ti : Sapphire Chameleon Ultra II laser (Coherent Inc.) was tuned to 750–800 nm and an Olympus XLUMPlanFI 20× objective (water immersed, numerical aperture, 0.95) was used for TPLSM imaging. To visualize infiltrating T cells in the dorsal spinal SAS, time-lapse sequences were performed at 70 µm stack height (2.5 µm z step) at

35–40 s intervals as previously described (17). Immediately after the first acquisition, 200 µl of artificial CSF containing 100 µg/ml of blocking anti- $\alpha 4$ integrins (clone PS/2, rat anti-mouse) or blocking anti- $\alpha 4\beta 7$ integrin (clone DATK32, rat anti-mouse) were locally applied to the exposed spinal cord and incubated for 30 min before a second round of imaging, to allow adequate local meningeal diffusion (17, 23–26).

TPLSM data analysis

Tracks longer than 3 min (≥ 12 time points) were manually tracked overtime from multidimensional rendering obtained by Imaris software (Bitplane) as previously described (17). Cell velocity and arrest index were computed. Track velocity was obtained from the mean instantaneous velocity calculated from all time intervals throughout a track. The arrest index represented the proportion of time during tracking in which a cell does not move (threshold ≤ 2 µm/min) and was calculated from cell tracks, so the reported value represents a percentage of cells in the entire population. The displacement of a cell moving with a constant velocity from an initial position, but randomly changing direction, was on average linearly proportional to the square root of the elapsed time (22).

EAE induction and antibody treatment

C57BL/6J females (8–10 weeks old) were immunized subcutaneously in the flanks with 100 µg of MOG₃₅₋₅₅ peptide in 200 µl emulsion containing phosphate-buffered saline (PBS) and complete Freund's adjuvant (CFA; Difco Laboratories) in equal volumes, supplemented with 0.8 mg/mouse *Mycobacterium tuberculosis* strain H37Ra (Difco Laboratories). Mice were treated with 25 ng of pertussis toxin (Alexis Biochemicals) intravenously at the time of immunization and 48 h later. Clinical scores were recorded daily as previously described (27).

Anti- $\alpha 4\beta 7$ treatment was administered intracisternally one day after the appearance of the first clinical signs and two days later with 50 µg of anti- $\alpha 4\beta 7$ (clone DATK32, rat anti-mouse) or control antibody (clone Y13-259, rat anti-human/mouse/rat). Each mouse was anesthetized and the atlanto-occipital membrane was punctured with a Hamilton syringe fitted with a 27-gauge needle containing 10 µl of antibodies solution (1.4 mg/ml corresponding to 50 µg antibody in approximately 35 µl of CSF) (28). We exclude potential interference with CNS leukocyte recruitment by antibody efflux from the CSF to periphery as discussed in our previous studies (17).

Neuropathology

After 3 days from the first intrathecal antibody injection, EAE mice were euthanized for spinal cords explant and freezing. 20-µm sections were used for inflammatory infiltrates investigation by hematoxylin/eosin (29) and the area covered by infiltrating leukocytes was expressed as % of the total white matter area.

Demyelination was evaluated by immunofluorescence staining with a purified anti-MBP antibody (clone D8X4Q, Cell Signaling), with DAPI as a nuclear co-stain. For the quantification of neuropathological findings, different lumbar and thoracic levels were evaluated on 4–6 cross-sections per mouse and results were expressed as a percentage of white matter area or total area, respectively (30).

For the quantification of infiltrating CD3⁺ cells, frozen sections of spinal cord were stained with an Alexa488-conjugated anti-CD3 antibody (clone 17A2, Biolegend) diluted 1:700, with DAPI as a nuclear co-stain. Results were represented as the area (μm^2) of fluorescent CD3⁺ cells relative to the total spinal cord area. All images were captured using Axio Imager Z2 (Zeiss, Germany) and interactively quantified using Intellesis module of Zen 2.6 Lite after supervised training of the machine learning system.

Statistics

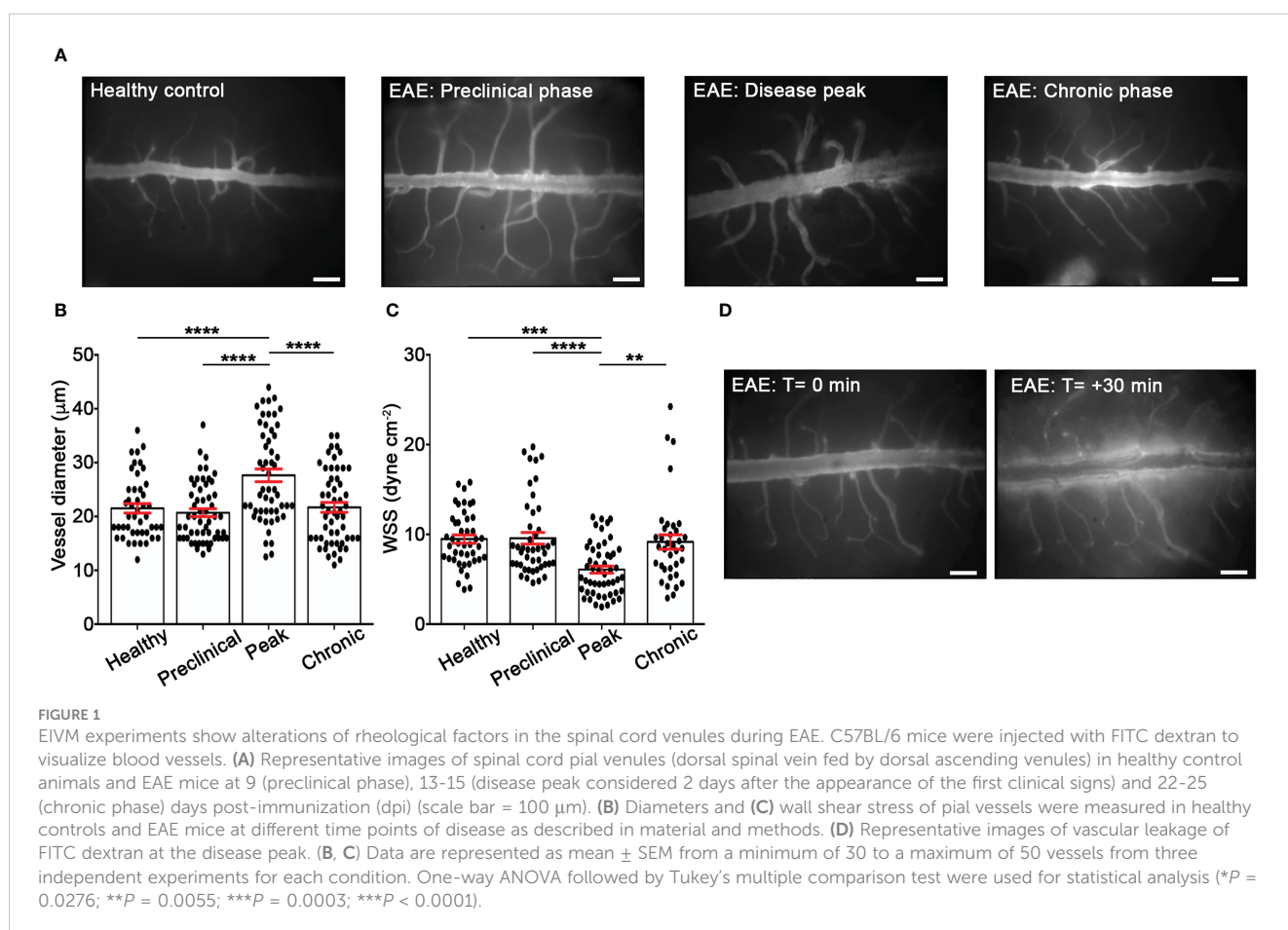
Data from flow cytometry, EIVM and TPLM studies are expressed as means \pm standard deviation (SD) or standard error of the mean (SEM). Statistical significance of data from flow cytometry and TPLM was calculated using the Mann–Whitney *U*-test, with a confidence interval of 95%. Outliers identification was calculated by Grubb's test with a *P* value < 0.05 considered as

statistically significant. Data from EIVM experiments were evaluated by ordinary one-way ANOVA followed by Dunnett's multiple comparison. In the plots of displacement, we applied linear regression and compared the slopes.

Results

Hemodynamic factors are altered in the spinal cord pial vessels during EAE

Rheological conditions have been shown to influence leukocyte and endothelium deformability, stiffness and activation and, consequently, leukocyte migration phenomena such as margination, rolling, integrin activation and diapedesis (31–33). To check the hemodynamics in EAE *versus* healthy mice, we performed laminectomy at the level of the lumbar spinal cord to visualize pial microcirculation. Our data clearly showed vasodilation and increased vessel diameter at disease peak compared with healthy animals, whereas no changes were observed at other disease time points (Figures 1A, B). In addition, we obtained results showing a reduction of wall shear stress (WSS) at disease peak compared to healthy mice and other disease conditions, further supporting an altered hemodynamic environment by acute/subacute inflammatory events during early



clinical disease (Figure 1C). Furthermore, we observed a significant vascular leakage of the fluorescent tracker at disease peak, indicating profound inflammatory vascular changes potentially accompanied by leukocyte adhesion phenomena (Figure 1D).

Th1 and Th17 cells have different adhesion capabilities in inflamed spinal cord pial vessels

Th1 and Th17 cells are potent inducers of autoimmunity and inflammation, and we next studied their adhesion capabilities in inflamed spinal cord leptomeningeal venules at different disease time points. By using flow cytometry analysis, we first studied the adhesive molecule expression of *in vitro* polarized MOG₃₅₋₅₅-specific Th1 and Th17 cells in terms of percentage of positive cells and mean fluorescence intensity (MFI). The following adhesion molecules were investigated: α 4 integrin chain, α 4 β 7 and LFA-1 integrins, CD44, L-selectin and PSGL-1 mucin. Th17 cells showed a significantly lower expression of L-selectin (70.8% for Th1 versus 32.5% for Th17 cells, $P = 0.0024$) and higher levels of CD44 integrin (MFI 35.7 for Th1 cells versus 62.3 in Th17 cells, $P = 0.0452$) suggesting a higher activation state compared to Th1 cells. Moreover, the percentage of Th17 cells expressing α 4 β 7 integrin was higher compared to Th1 cells (54% for Th17 cells versus 31.4% for Th1 cells, $P = 0.0196$) (Supplementary Figure 1; Supplementary Table I), suggesting a potential role for this adhesion molecule in Th17 cell adhesion. LFA-1 was more expressed on Th1 cells compared to Th17 cells, further suggesting different adhesion potential and extravasation capacity of these two T cell types in the inflamed target tissue.

In order to investigate the adhesion of MOG₃₅₋₅₅-specific Th1 and Th17 cells in the spinal SAS venules, we next performed EIVM experiments at different time points after EAE induction by simultaneous injection of Th1 and Th17 cells labelled with different fluorescent dyes. Particularly, we investigated T cell adhesion events in the pre-clinical phase at nine days post immunization (dpi), at disease peak (13–15 dpi), which was considered at two days after the onset of clinical signs, and during the chronic phase (22–25 dpi). Th1 cells showed a higher capacity to roll on pial vessel endothelium (26.5% versus 19.4%, $P = 0.0172$) and arrest (4.4% versus 1.4%, $P = 0.0026$) in leptomeningeal venules when compared to Th17 cells at the preclinical phase of disease. Conversely, at disease peak, Th17 cells were more adhesive when compared to Th1 cells, presenting a more efficient capacity to roll (26.1% versus 21.0% respectively, $P = 0.0412$) and arrest (3.8% versus 2.2% respectively, $P = 0.0419$). EIVM experiments performed during the chronic phase showed that Th1 and Th17 cells display a similar capacity to arrest in the spinal pial venules (2.3% versus 2.8%, $P = 0.3705$), although Th1 cells had a higher tendency to roll compared to Th17 cells (25.5% versus 20.0%, $P = 0.0131$) (Figure 2A, B; Supplementary Table II). Together, these data suggest a phase-specific adhesion capacity of Th1 and Th17 cells in disease development in EAE mice, prompting us to hypothesize a role for integrins in this phenomenon potentially relevant for the development of CNS inflammation.

LFA-1 and α 4 β 7 integrins have differential roles in Th1 and Th17 cell adhesion in leptomeningeal venules during EAE

We next evaluated the role of LFA-1 and α 4 integrins in MOG₃₅₋₅₅-specific Th1 and Th17 cell adhesion in spinal pial venules by performing EIVM experiments at different time points of EAE. T cell pre-treatment with an anti-LFA-1 blocking antibody led to a strong inhibition of both rolling and arrest of Th1 cells in the preclinical phase of EAE (57% blockade of rolling, $P = 0.0030$ and 87.5% inhibition of arrest, $P = 0.0001$). However, LFA-1 blockade had a less impact on adhesion interactions at disease peak and had no significant effect during the chronic phase, suggesting a prominent role for this integrin in Th1 cell migration during early EAE (Figure 2C; Supplementary Table III). Notably, LFA-1 blockade did not significantly affect the adhesive interactions between Th17 cells and vascular endothelium in the spinal SAS during all examined time points, demonstrating the existence of specific molecular mechanisms controlling Th1 versus Th17 cell adhesion in inflamed leptomeningeal vessels during EAE (Figure 2D; Supplementary Table IV). An isotype control antibody had no effect on the adhesion events of both Th1 and Th17 cells (data not shown).

We also determined the role of α 4 integrins in EIVM experiments by using blocking anti- α 4 or anti- α 4 β 7 antibodies. In the preclinical phase of disease, α 4 chain blockade in Th1 cells inhibited approximately 60% of rolling and arrest events ($P = 0.0027$ and $P = 0.0023$ for rolling and arrest, respectively) (Figure 3A), whereas, in contrast, had no effect on Th17 cell adhesion (Figure 3B). Furthermore, α 4 β 7 integrin blockade did not affect Th1 cell adhesiveness, suggesting VLA-4/ α 4 β 1 as the specific α 4 integrin involved in Th1 cell rolling and adhesion in spinal pial vessels at the preclinical phase of disease (Supplementary Figure 2). At disease peak, α 4 blockade led to a substantial reduction of rolling (73% inhibition, $P < 0.0001$) and arrest (81% inhibition, $P < 0.0001$) (Figure 3A) in Th1 cells. However, α 4 β 7 blockade at the same time point of disease had no effect on Th1 adhesion, clearly indicating the predominant role of VLA4 integrin in Th1 cell intravascular adhesion during early clinical disease. Interestingly, α 4 chain inhibition in Th17 cells massively reduced the arrest (87% inhibition, $P = 0.0006$), but had no effect on rolling, suggesting that different α 4 integrins may control adhesion interactions in Th1 versus Th17 cells in inflamed leptomeningeal vessels (Figure 3B). Indeed, selective α 4 β 7 blockade drastically inhibited the arrest (74% inhibition, $P = 0.0037$) without interfering with rolling, demonstrating a clear overlap with the results obtained with the anti- α 4 chain blocking antibody and indicating a crucial role for α 4 β 7 in Th17 cell adhesion in SAS vessels. Finally, we studied the adhesion interactions during the chronic phase of disease and observed that the pretreatment of Th1 cells with the anti- α 4 chain antibody inhibited 46% of rolling ($P = 0.0290$) and almost completely abrogated the arrest (94% of inhibition, $P < 0.0001$). As also shown for the disease peak, α 4 β 7 blockade had no effect on adhesion interactions, further supporting a pivotal role for VLA-4 in Th1 cell migration in the animal model of MS (Figure 3A; Tables III, IV). When we studied Th17 cell adhesion, we observed that the blockade of both α 4 chain and α 4 β 7 integrin dimer led to a drastic

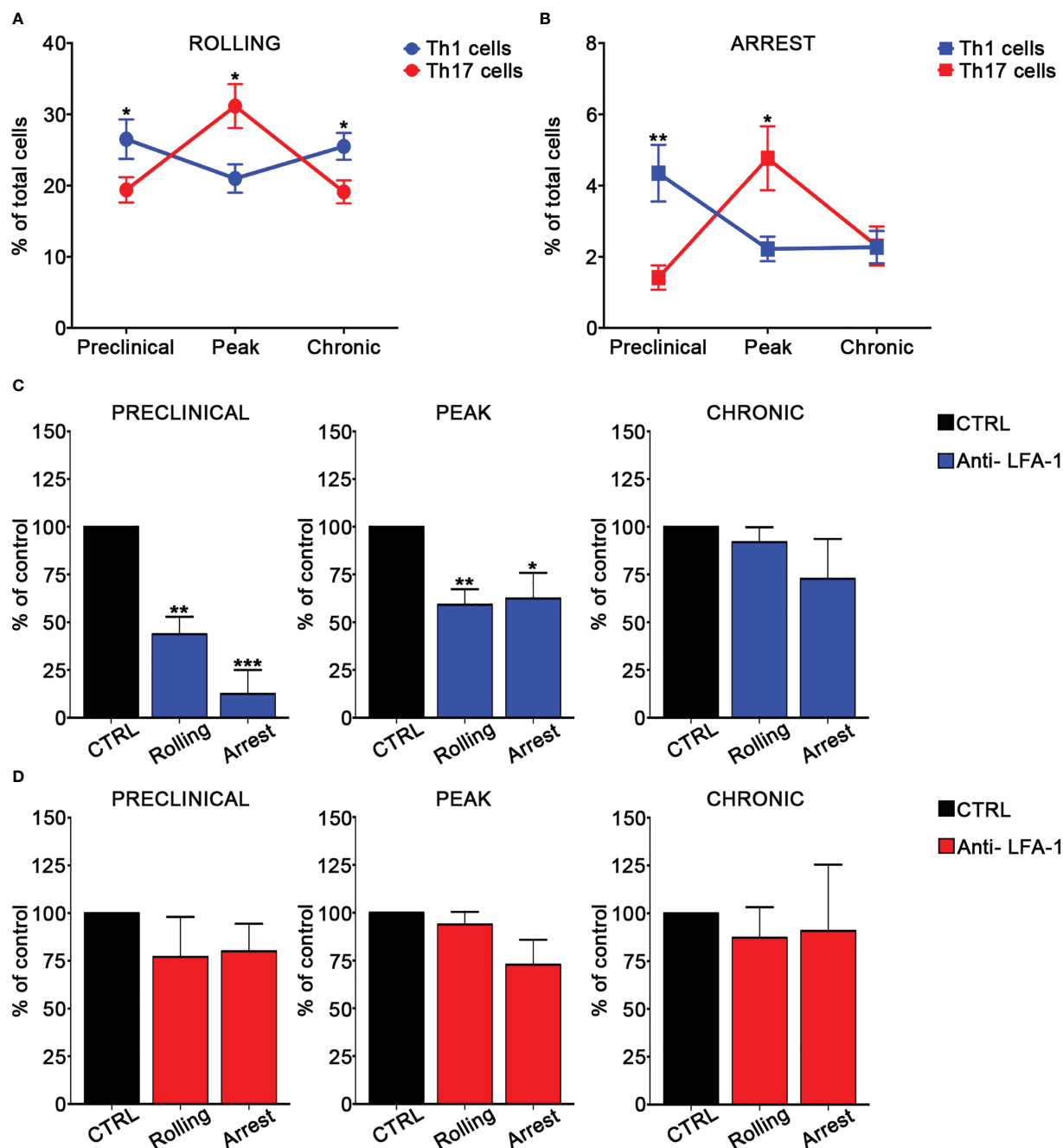
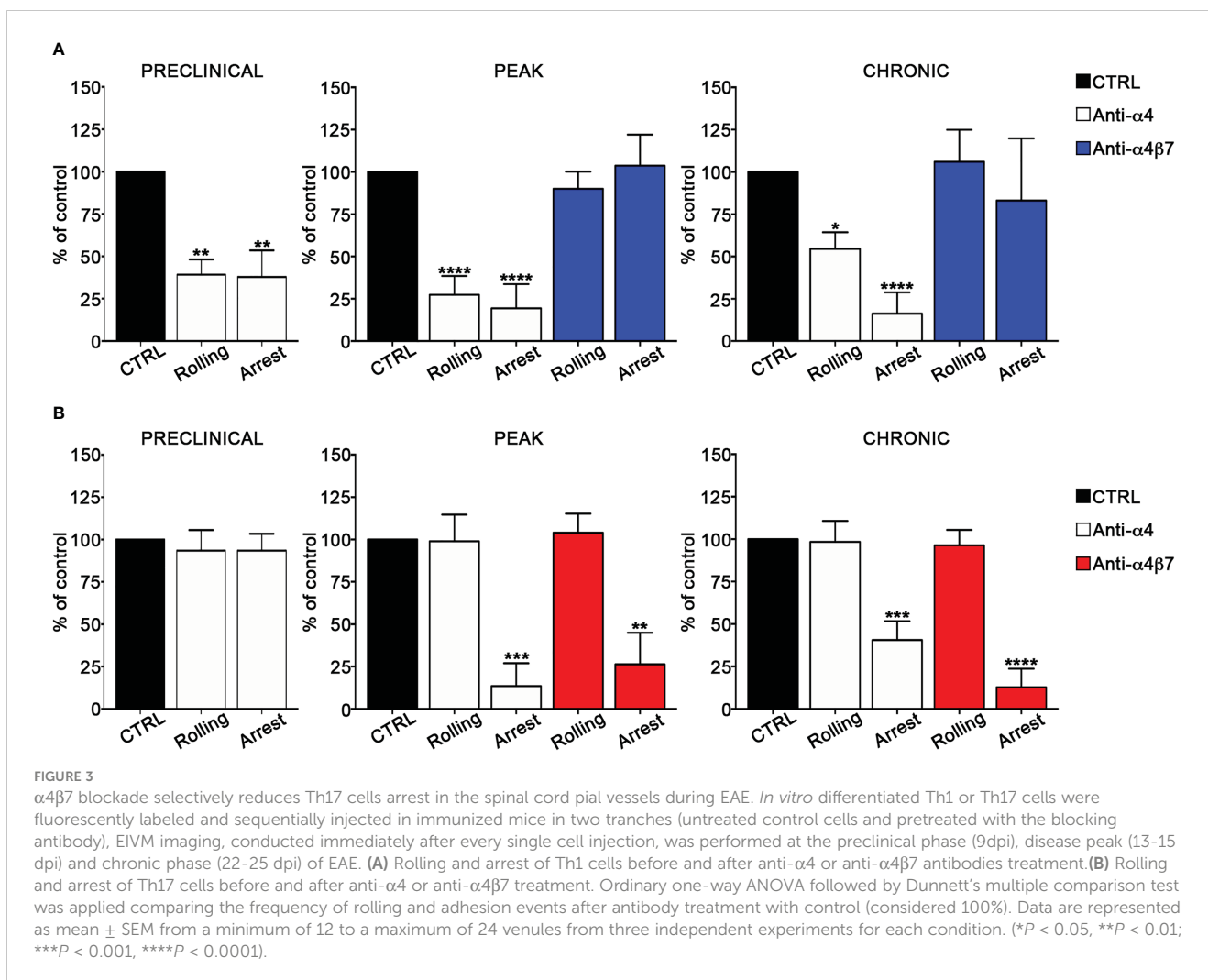


FIGURE 2
 Th1 and Th17 rolling and arrest in spinal cord pial vessels during EAE. (A, B) *In vitro* differentiated Th1 and Th17 cells were fluorescently labeled and co-injected in immunized mice immediately before EIVM imaging at different time point of EAE. The percentage of rolling (A) and arrest (B) of Th1 and Th17 cells was evaluated as described in material and methods. Differences in terms of percentage of rolling and adhesion between Th1 and Th17 cells at different time points were determined by using Mann-Whitney *U* test (one tailed). Data are expressed as mean \pm SEM from three independent experiments for each time point during EAE. (* $P < 0.05$; ** $P = 0.0026$). (C, D) *In vitro* differentiated Th1 or Th17 cells were fluorescently labeled, divided in two groups (untreated control cells and pretreated with the anti-LFA-1 antibody) and sequentially injected in immunized mice at different time points of EAE. EIVM imaging was performed immediately after every single cell injection at different time points of EAE. (C) Rolling and arrest of Th1 cells treated or not (CTRL) with anti-LFA-1 antibody at the preclinical phase, disease peak (2 days after the appearance of the first clinical signs) and chronic EAE. (D) Rolling and arrest of Th17 cells treated or not (CTRL) with anti-LFA-1 antibody at the preclinical phase, disease peak and chronic phase of EAE. One-way ANOVA followed by Dunnett's multiple comparison test was applied to compare the frequency of rolling and adhesion events after antibody treatment with of untreated control cells (considered 100%). Data are represented as mean \pm SEM from a minimum of 10 to a maximum of 19 venules from three independent experiments for each condition. (* $P < 0.05$, ** $P < 0.01$; *** $P < 0.001$).



inhibition of arrest (60% inhibition, $P = 0.0001$ in the case of anti- $\alpha 4$ antibody and 88% inhibition, $P < 0.0001$ after $\alpha 4\beta 7$ integrin blockade), further demonstrating the importance of $\alpha 4\beta 7$ in Th17 cell stable adhesion (Figure 3B; Tables III, IV). The number of adhering controls Th17 cells during all EAE phases was generally low (from 1.1% of the total number of analyzed cells per vessel at the preclinical phase to 5.5% at the disease peak, (Supplementary Table IV) suggesting that Th17 cell arrest is tightly regulated. This observation, together with the strong inhibition exerted by $\alpha 4\beta 7$ blockade, highlight the crucial role of $\alpha 4\beta 7$ integrin in Th17 cell arrest in spinal leptomeningeal vessels. Collectively, these data also highlight a different usage of $\alpha 4$ integrins in T cell adhesion in inflamed leptomeningeal vessels, with VLA-4/ $\alpha 4\beta 1$ integrin being crucial for Th1 cells and $\alpha 4\beta 7$ integrin having a pivotal role for Th17 cells.

$\alpha 4\beta 7$ integrin selectively controls Th17 cell motility in the spinal SAS during EAE

To further understand the role of integrins in MOG_{35–55}-specific Th1 and Th17 cell migration during EAE, we next

determined the role of $\alpha 4$ integrins in the dynamics of extravasated Th1 and Th17 cells in the spinal SAS. Previous results obtained by our laboratory demonstrated that Th1 and Th17 cells massively infiltrate leptomeninges at disease peak during EAE showing significant differences in their motility behavior and suggesting distinct molecular mechanisms controlling their dynamics (17). In light of these data, we performed TPLSM experiments to evaluate the role of $\alpha 4$ integrins in the motility of Th1 and Th17 cells at disease peak. Particularly, we intravenously injected fluorescently labelled Th1 or Th17 cells into EAE mice at disease onset and, after 48 h when mice reached the disease peak. As previously shown for LFA-1 and $\alpha 4$ integrins (17), $\alpha 4\beta 7$ expression was maintained on transferred exogenous T cells after migration into the spinal cord, with Th17 cells having a higher expression of this integrin compared to Th1 cells (Figure 4A). To check if our *in vitro* differentiated T cells mimic the expression of $\alpha 4\beta 7$ on endogenous cells, we evaluated $\alpha 4\beta 7$ expression on endogenous Th1 and Th17 cells in the blood and spinal cord of EAE mice at disease peak. We identified CXCR3+ CCR4- CCR6- as Th1 cells and CXCR3- CCR4+ CCR6+ as Th17 cells (34). Our data confirmed that also endogenous Th17 cells have a higher $\alpha 4\beta 7$ integrin expression

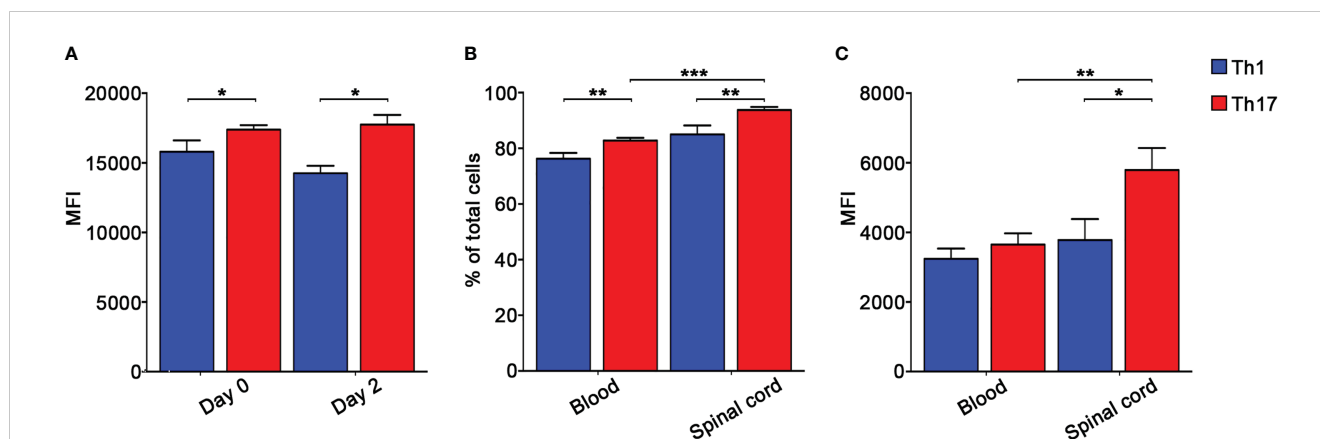


FIGURE 4

Endogenous and *in vitro* polarized Th17 cells express higher levels of $\alpha 4\beta 7$ integrin compared to Th1 cells. (A) CMAC-labelled *in vitro* polarized Th1 or Th17 cells were intravenously injected into different EAE recipient mice at disease onset and harvested from the spinal cord 48 hours later. $\alpha 4\beta 7$ integrin expression by Th1 (blue) and Th17 (red) cells was evaluated before and after cell transfer and shown as MFI. Data are expressed as mean \pm SEM from 3–4 mice for each Th cell subset. Statistical significance was calculated using the Mann–Whitney test (* $P < 0.05$). Endogenous Th cell subpopulations were identified according to their chemokine receptors expression patterns. Particularly, CXCR3+ CCR4- CCR6- CD4+ T cells were classified as Th1 cells, whereas CXCR3- CCR4+ CCR6+ CD4+ T cells were classified as Th17 cells. (B) The percentages of $\alpha 4\beta 7$ integrin-expressing endogenous circulating and spinal cord-infiltrating Th1 (blue) and Th17 (red) cells were evaluated by flow cytometry after surface staining. Data are expressed as mean \pm SEM from 5–8 mice. Statistical significance was calculated using the Mann–Whitney test (** $P < 0.01$; *** $P < 0.001$). (C) MFI shows that endogenous spinal cord infiltrating Th17 cells display the highest level of $\alpha 4\beta 7$ integrin. Data are expressed as mean \pm SEM from 5–8 mice. Statistical significance was calculated using the Mann–Whitney test (* $P < 0.05$; ** $P < 0.01$).

compared to Th1 cells in terms of both percentage of expressing cells and MFI (Figures 4B, C).

Our TPLSM experiments comparing cell motility before and after direct application of blocking antibodies on the exposed spinal cord, demonstrated no significant differences in the dynamics of Th1 cells before and after local $\alpha 4$ chain blockade, as shown by the measurements of mean velocity (3.8 versus 3.6 $\mu\text{m}/\text{min}$, $P = 0.3622$), arrest coefficient (0.31 versus 0.35, $P = 0.0590$) and displacement (curve slope: 6.7 versus 7.5, $P = 0.0884$) (Figure 5; Supplementary Movie 2), clearly indicating that $\alpha 4$ integrins are not involved in the locomotion of Th1 cells inside the spinal SAS of EAE mice. However, Th17 cells showed a significant motility reduction after $\alpha 4$ integrin blockade, as proved by the results on the Th17 cell speed (from 4.7 to 3.0 $\mu\text{m}/\text{min}$, $P = 0.0095$) (Figure 6C) and arrest index (0.23 versus 0.34, $P = 0.0149$) (Figure 6D). Moreover, Th17 cells showed a significant reduction in the curve slope (from 7.5 to 4.3, $P = 0.0072$), indicating that $\alpha 4$ integrin blockade interferes with their capacity to travel for long distances and cover large tissue volumes (Figures 6A, B, E). To unveil a potential role for $\alpha 4\beta 7$ in Th17 cell motility in the spinal SAS, we next performed TPLSM experiments by directly applying a blocking anti- $\alpha 4\beta 7$ antibody on the exposed spinal cord. Notably, our results clearly showed a strong reduction in the movement velocity of Th17 cells after $\alpha 4\beta 7$ blockade (5.0 versus 4.0 $\mu\text{m}/\text{min}$, $P < 0.0001$), an increment of the arrest index (from 0.28 to 0.43, $P < 0.0001$) and a decrease of the slope of displacement curve (from 7.8 to 5.4, $P < 0.0001$), strongly indicating a major role for $\alpha 4\beta 7$ integrin in the locomotion of Th17 cells inside the spinal SAS during EAE (Figure 7; Supplementary Movie 3). However, in the present study we observed some differences in the velocity of Th cells comparing to our previous data (17), probably due to variability in meningeal inflammation between mice and the fact that in this work we did not co-inject Th1 and Th17 cells in the same animals.

Intrathecal $\alpha 4\beta 7$ blockade inhibits the development of EAE

We have previously shown that interfering with autoreactive T cell motility hampers detrimental T cell activities and, consequently, attenuates EAE development (17). To determine the therapeutic effect of $\alpha 4\beta 7$ integrin blockade on extravasated Th17 cell motility inside the spinal SAS, we intrathecally injected two doses of an anti- $\alpha 4\beta 7$ antibody in EAE mice after the clinical onset (one day after the appearance of the first clinical signs and two days later). These doses were higher than the saturating dose of anti- $\alpha 4\beta 7$ mAb found in our previous flow cytometry studies (data not shown). $\alpha 4\beta 7$ blockade led to a statistically significant reduction in disease severity compared to a control antibody, and the effect lasted at least two weeks after treatment termination ($P = 0.0461$) (Figure 8A). Disease amelioration was associated with a marked reduction in the demyelination ($P < 0.0001$) and inflammatory cell infiltration ($P < 0.0001$) in the anti- $\alpha 4\beta 7$ treated animals compared to isotype control treated mice (Figures 8B, C). Also, we found a significant reduction in the CD3⁺ cell compartment ($P < 0.0001$), suggesting that intrathecal $\alpha 4\beta 7$ blockade also reduces T cell invasion of the CNS, attenuating the neuroinflammatory environment (Figure 8D).

Discussion

MS and its experimental models are complex and heterogeneous chronic inflammatory disorders of the CNS with several immune cell populations involved in disease pathogenesis, including Th1 and Th17 cells (18, 35, 36). Indeed, previous studies suggested that disease heterogeneity in terms of different clinical course, CNS lesion distribution in the brain versus spinal cord and

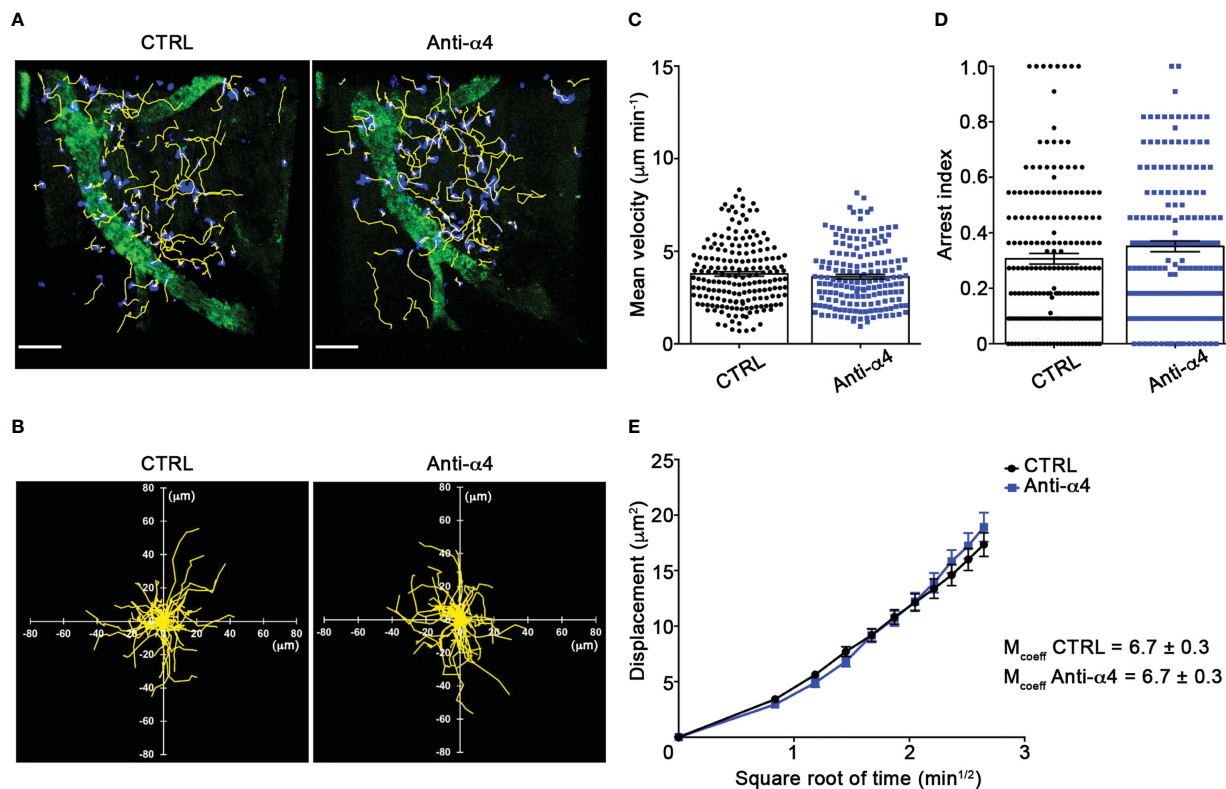


FIGURE 5

$\alpha 4$ integrins do not affect Th1 cells motility behavior in the spinal SAS at EAE peak. *In vitro* differentiated Th1 cells were fluorescently labeled and intravenously injected at disease onset. TPLSM imaging was performed after 48 h, when mice reached the disease peak. (A) Representative images of Th1 cells moving in the spinal SAS before (CTRL) and after 30 min of anti- $\alpha 4$ integrin treatment (anti- $\alpha 4$ antibody) (scale bar = 50 μm). (B) Normalized trajectories of 70 Th1 cells over 12 time points before and after anti- $\alpha 4$ antibody. (C) Mean velocity and (D) arrest index of Th1 cells before and after $\alpha 4$ integrins blockade. Statistical significance was calculated using the Mann-Whitney test. (E) Mean displacement of Th1 cells in not affected by anti- $\alpha 4$ blocking antibodies (After linear regression application, the differences between slopes resulted not quite significant; $P = 0.0884$). All data are expressed as mean \pm SEM. A total of 185 cells were analyzed for CTRL and 171 after anti- $\alpha 4$ treatment from two independent experiments. Track lower than 12 time points were excluded from the analysis.

response to immunomodulatory therapies, may depend on whether the predominant immune response is mediated by Th1 or Th17 cells (35, 37–45).

Both human and murine Th1 and Th17 cells express different patterns of adhesion molecules and chemokine receptors that can influence the preferential accumulation of these cells in the brain or spinal cord (35). VLA-4 is considered the major integrin controlling the accumulation of Th1 cells in the CNS (46), while LFA-1 was shown to control Th17 cell recruitment into the brain in the absence of functional $\alpha 4$ integrins (47). Thus, the relative levels of integrin expression on Th1 and Th17 cells may support different patterns of migration and inflammation, leading not only to the preferential localization of these cells in the spinal cord *versus* brain, but also indirectly impacting the subsequent recruitment of other immune cell types contributing the inflammatory responses. Our *in vitro* polarized MOG₃₅₋₅₅-specific Th17 cells had higher expression of CD44 and lower L-selectin expression, supporting an increased ability to invade non-lymphoid inflamed tissues (48, 49). Notably, the percentage of Th17 cells expressing $\alpha 4\beta 7$ integrin was significantly higher compared to Th1 cells, and these data are supported by previous studies showing that $\alpha 4\beta 7^{\text{hi}}$ CD4⁺ T cells harbor most Th17 cells during viral infection (50). We did not find

differences in the expression of $\alpha 4$ integrin chain between Th1 and Th17, as also supported by other studies (51). However, data obtained by Rothhammer et al. found a higher $\alpha 4$ integrin expression on *in vitro* differentiated Th1 cells compared to Th17 cells (47). This may be explained by a different *in vitro* protocol, in which Th cells were differentiated by a single polyclonal stimulation without subsequent cell amplification, whereas in our manuscript, as well as in other studies, naïve CD4⁺ T cells were primed with MOG₃₅₋₅₅ twice followed by cell amplification with cytokines (47, 51). In our experimental setting, *in vitro* differentiated Th17 cells showed higher expression of $\alpha 4\beta 7$ integrin compared to Th1 cells, and this difference was also found on endogenous Th cells migrated into the spinal cord, suggesting that our experimental system could mimic the motility capability of Th1 and Th17 cells during EAE, as also previously demonstrated by our group (17). The higher expression of $\alpha 4\beta 7$ on exogenous transferred Th17 cells may be explained by the stronger activation induced by *in vitro* polarization, making them less responsive to the local inflammatory milieu, as indicated by their unperturbed integrin profile after 48 hours of *in vivo* migration. In addition, the lower expression of $\alpha 4\beta 7$ on endogenous Th17 cells could be due to a more heterogenous state of activation of these cells during EAE.

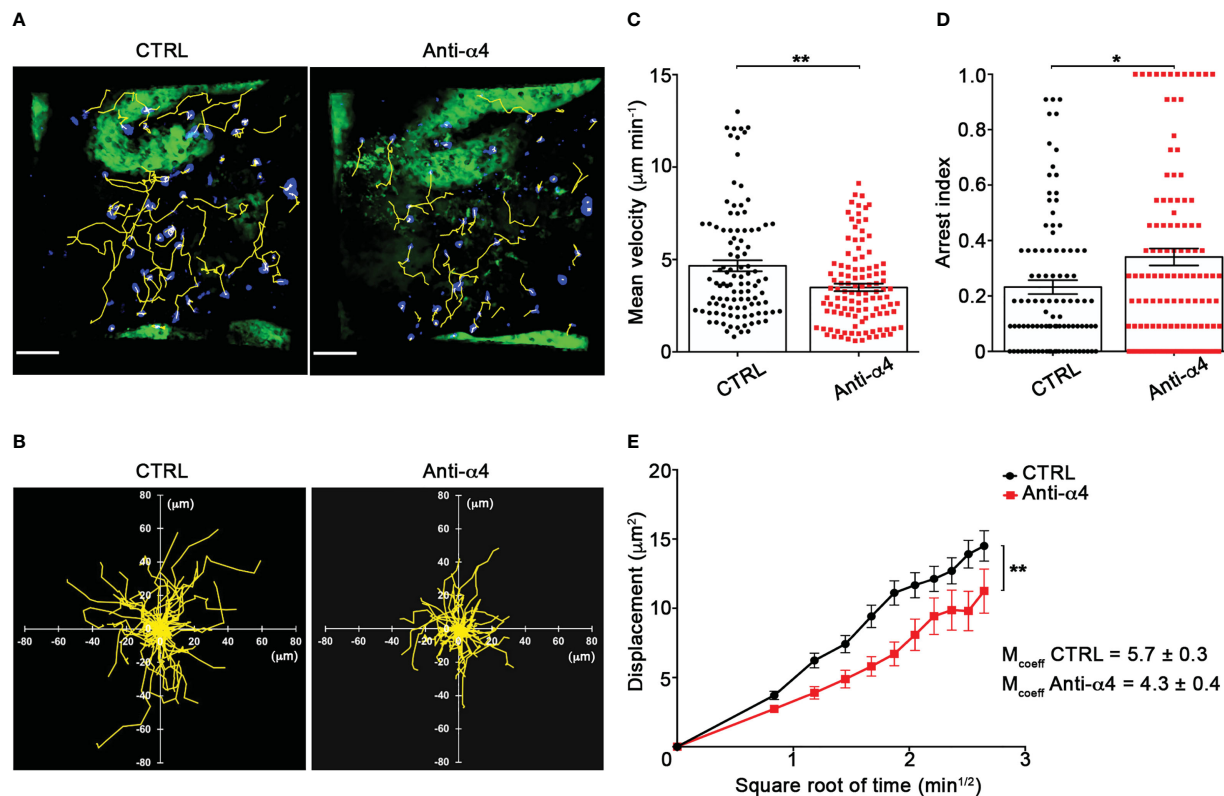


FIGURE 6

$\alpha 4$ integrins control Th17 cells motility in the spinal SAS at disease peak. *In vitro* differentiated Th17 cells were fluorescently labeled and intravenously injected at disease onset. TPLSM imaging was performed after 48 h, when mice reached the disease peak. (A) Representative images of Th17 cells before (CTRL) and after 30 min of anti- $\alpha 4$ integrin treatment (anti- $\alpha 4$ antibody) (scale bar = 50 μm). (B) Normalized trajectories of 70 Th17 cells before and after anti- $\alpha 4$ antibody. (C) Mean velocity (** $P = 0.0095$) and (D) arrest index (** $P = 0.0149$) of Th17 cells before and after $\alpha 4$ integrin blockade. Statistical significance was calculated using the Mann–Whitney test ($*P < 0.05$). (E) Mean displacement of Th1 cells is significantly reduced after anti- $\alpha 4$ blocking antibodies (After linear regression application, the differences between slopes resulted statistically significant; ** $P = 0.0072$). All data are expressed as mean \pm SEM. A total of 104 cells were analyzed for CTRL and 111 after anti- $\alpha 4$ treatment from two independent experiments. Track lower than 12 time points were excluded from the analysis.

However, $\alpha 4\beta 7$ expression on migrated endogenous Th17 cells is drastically enhanced by the spinal environment.

Contradictory data have been published on the sequence of Th1 and Th17 cell entry into the CNS during EAE development. Previous reports suggested that Th1 cells entry into the CNS is required to facilitate subsequent wave of Th17 cell migration (52), whereas other studies found that Th17 cells are the earliest subpopulation infiltrating the CNS in the pre-clinical phase, with Th1 cells accumulating later at disease onset (53, 54). Most likely, the collection of these data in EAE mice was influenced by the high *in vivo* plasticity shown by Th1 and Th17 cells (55–57). To overcome the limitation of a potential *in vivo* phenotype change, we used *in vitro* differentiated MOG₃₅₋₅₅-specific Th1 and Th17 cells and studied their adhesion in short term assays in EIVM experiments immediately after intravenous injection. Also, MOG₃₅₋₅₅-specific Th1 and Th17 cells were used in TPLSM studies within 2 days after injection, when these cells maintain their initial phenotype as previously described (17).

Whereas T cell accumulation was mainly investigated in the brain and spinal cord of EAE mice, growing evidence highlight a key role for the meningeal space in driving parenchymal immune

cell invasion and inflammation in EAE and MS (10, 58–60). However, the molecular mechanisms controlling rapid adhesion events such as tethering, rolling and arrest in spinal cord leptomeninges as well as the migration behavior in the meningeal space during EAE are not well elucidated. In this manuscript we studied the ability of MOG₃₅₋₅₅-specific Th1 and Th17 cells to interact with endothelium in spinal cord pial venules at different phases of EAE and our data found clear differences between these two cell populations, suggesting distinct molecular mechanisms regulating their extravasation into the meninges. Indeed, Th1 cells showed higher rolling and arrest capacity than Th17 cells during the preclinical phase of EAE, pointing to a prominent role for Th1 cells in leptomeningeal inflammation during early EAE. IFN- γ produced by Th1 cells may induce expression of adhesion molecules and tight junctions alterations, facilitating the migration of subsequent inflammatory cells as demonstrated by other studies (61–63). At disease peak, Th17 cells displayed a significantly higher capacity to perform arrest, suggesting a pathological role for Th17 cells necessary for clinical disease progression. Indeed, previous studies have shown that IL-17A induces blood-brain barrier dysfunction, favoring ensuing transmigration of other lymphocyte

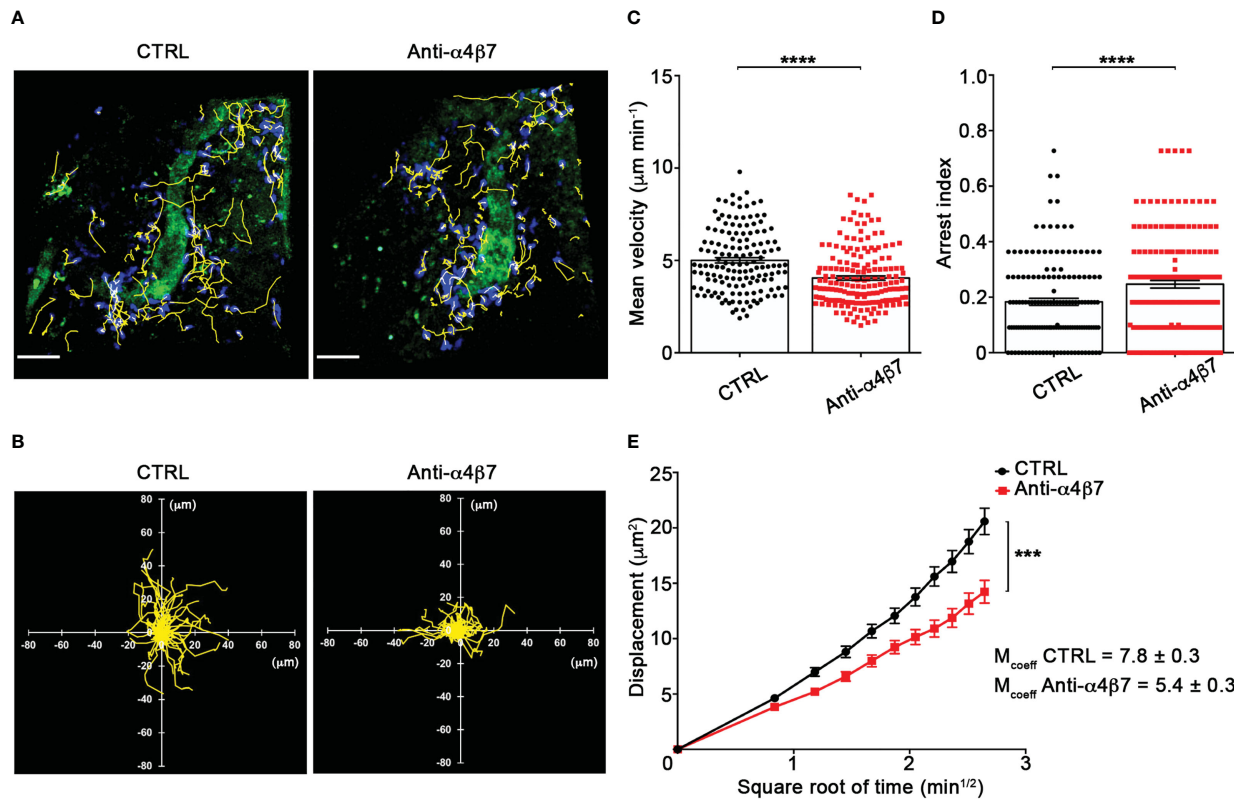
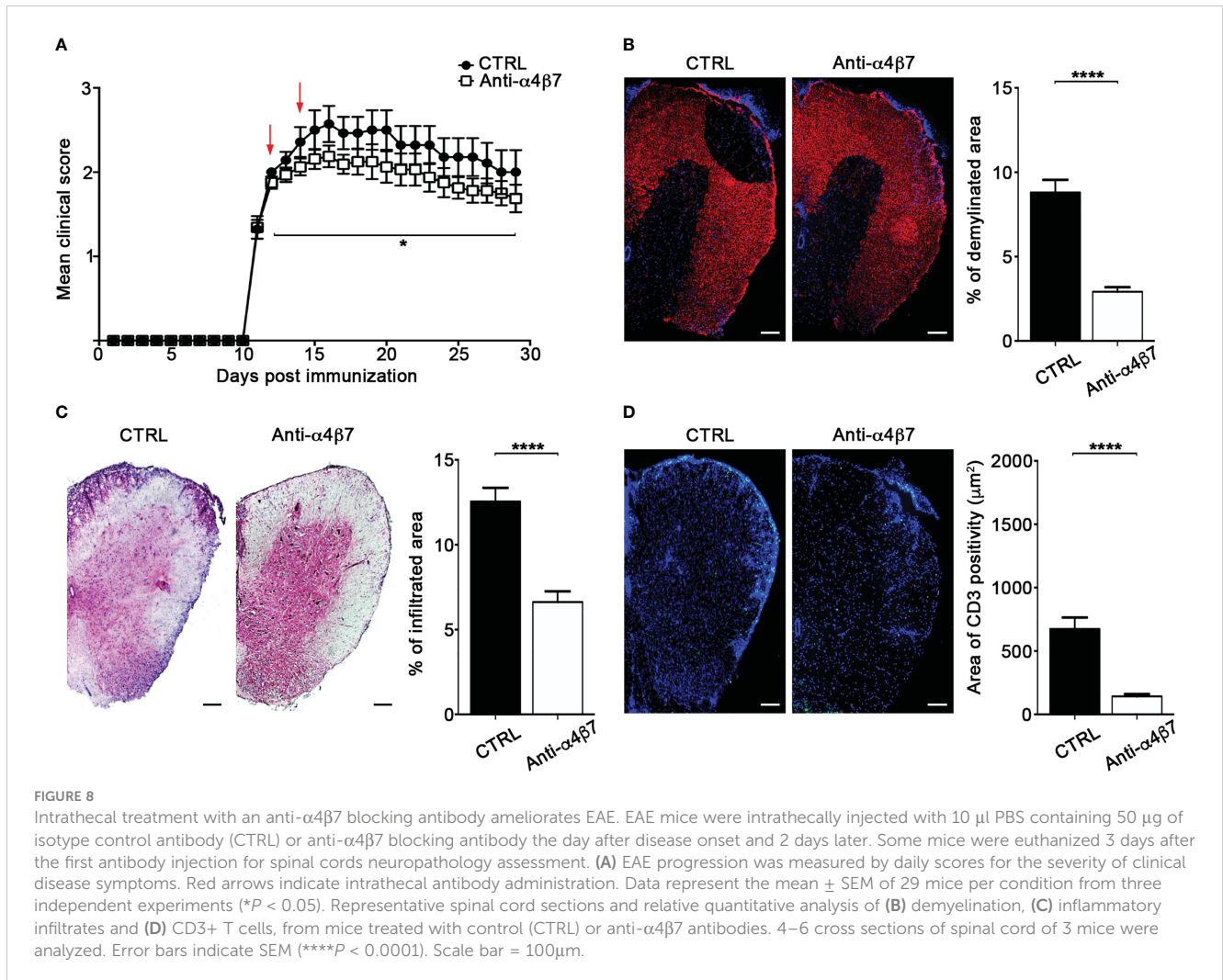


FIGURE 7
 $\alpha 4\beta 7$ integrin selectively controls Th17 cells dynamics in the spinal SAS at disease peak. Cell preparation and TPLSM imaging were performed as described for Figure 5. (A) Representative images of Th17 cells before (CTRL) and after 30 min of anti- $\alpha 4\beta 7$ integrin treatment (anti- $\alpha 4\beta 7$ antibody) (scale bar = 50 μm). (B) Normalized trajectories of 70 Th17 cells over 12 time points before and after anti- $\alpha 4\beta 7$ antibody. (C) mean velocity and (D) arrest index of Th17 cells before and after integrin blockade. Statistical significance was calculated using the Mann-Whitney test (**** $P < 0.0001$). (E) Mean displacement of Th17 cells is strongly decreased by anti- $\alpha 4\beta 7$ blocking antibodies (After linear regression application, the differences between slopes resulted extremely significant; **** $P < 0.0001$). Data are expressed as mean \pm SEM. A total of 146 cells were analyzed for CTRL and 176 after anti- $\alpha 4$ treatment from three independent experiments. Track lower than 12 time points were excluded from the analysis.

subpopulations, including Th1 cells, in the CNS (64–66). Vascular leakage observed in our study coincides with higher Th17 adhesion, further pointing to Th17 cells as key players in the progression of clinical disease. Some differences in rolling between Th1 and Th17 cells were observed during chronic EAE, but the arrest capacity was similar, suggesting that both cell types may contribute to chronic leptomeningeal inflammation.

Our data show that $\alpha 4$ integrins are key adhesion molecules mediating both rolling and arrest of Th1 cells in leptomeningeal vessels during all EAE phases (pre-clinical phase, disease peak and chronic phase), confirming the predominant role of $\alpha 4$ integrins in Th1 cell adhesion. Interestingly, blockade of $\alpha 4$ integrins in Th17 cells only reduced the arrest without interfering with rolling, suggesting these molecules may be differently distributed on the plasma membrane of Th17 cells compared to Th1 cells (67). Moreover, these data also hinted that distinct $\alpha 4$ integrins may be involved in Th17 versus Th1 cell adhesion in leptomeningeal vessels. Indeed, our results clearly showed that a blocking antibody against $\alpha 4\beta 7$ integrin strongly inhibited the adhesion of Th17 cells at disease peak and during the chronic phase, but had no effect on Th1 cells, unveiling a selective role for $\alpha 4\beta 7$ integrin in Th17 cell migration in leptomeningeal vessels. In support of our

data, a selective role for $\alpha 4\beta 7$ integrin in Th17 trafficking has also been shown in a murine model of autoimmune ocular inflammation (51). In addition, previous studies reported that in *Rag1*^{-/-} mice in which EAE was induced by a transfer of *in vitro* differentiated MOG₅₃₋₅₅-specific Th17 cells, systemic blockade of $\alpha 4$ integrins inhibited Th17 migration into the spinal cord parenchyma, but not the brain inducing signs of atypical EAE with ataxia and hemiparesis. These data were also confirmed in EAE mice by transferring $\alpha 4$ deficient Th17 cells. Interestingly in the same experimental setting, the interference with $\alpha 4$ integrin chain completely abrogated transferred Th1 cell accumulation in both spinal cord and brain reducing EAE manifestations and further supporting a role for $\alpha 4\beta 7$ integrin in Th17 cell migration during MOG₃₅₋₅₅-induced EAE (47). However, $\alpha 4$ integrins had no role in Th17 adhesion in leptomeningeal vessel during the preclinical phase of disease, suggesting that other molecules are responsible for the entry of Th17 in the spinal SAS during this disease phase. Interestingly, the adhesion interactions of Th17 cells were not affected by LFA-1 blockade during all disease phases, whereas Th1 cell adhesion was significantly reduced, further demonstrating relevant differences in the migration mechanisms between Th1 and Th17 subsets. Indeed, previous studies suggested



that LFA-1 may control Th17 migration into the brain, but not into the spinal cord, highlighting the complexity of Th cell recruitment process during EAE (47).

MAdCAM-1 is considered the high affinity ligand for $\alpha 4\beta 7$ integrin (68). It was shown to be expressed on inflamed CNS vessels in a chronic relapsing form of EAE, but its role in T cell migration during EAE is not well understood (69–71). Whereas in a model of relapsing–remitting EAE in SJL mice, blockade of $\beta 7$ integrins had no effect on disease (72), inhibition of MAdCAM-1 or $\beta 7$ integrins significantly interfered with disease development in a chronic EAE model in C57BL/6 mice, supporting our data obtained in the same experimental model (70, 73). Although with lower affinity than VLA-4, $\alpha 4\beta 7$ integrin can bind VCAM-1 (74), and we hypothesize that VCAM-1, which has a high endothelial expression in the CNS during MS and EAE, may represent an alternative endothelial counter-ligand in leptomeningeal vessels for $\alpha 4\beta 7$ integrin expressed on Th17 cells (75). Once migrated through the pial vessel wall, encephalitogenic T cells need to be reactivated by leptomeningeal APCs for acquiring the ability to infiltrate the CNS parenchyma (10, 76). In this context, T cell locomotion inside the SAS could be therefore of fundamental importance for

antigen scanning and contacts with resident cells. However, our understanding of activated T cell dynamics after extravasation into the CNS and meninges is still unclear. By using a TPLSM approach, we have previously shown two distinct LFA-1-dependent migratory patterns used by Th1 and Th17 cells, suggesting that different molecular mechanisms control intrameningeal locomotion during EAE (17). Also, our data demonstrated that interfering with T cell motility inside the spinal SAS reduces their pathogenic potential and mitigates EAE (17). In a murine model of autoimmune ocular inflammation, Cox and colleagues reported that *in vivo* reactivation leads to higher expression of $\alpha 4\beta 7$ and CCR6 in transferred Th17, but not Th1, cells, further emphasizing the importance of migration mechanisms in CD4+ cell pathogenicity (51). In our TPLSM experiments, Th1 motility behavior in the leptomeninges was independent of $\alpha 4$ integrins, whereas $\alpha 4$ integrin chain blockade led to a drastic reduction of Th17 cell locomotion in terms of mean velocity, arrest index and displacement in the spinal SAS at EAE peak. $\alpha 4\beta 7$ expression was higher on Th17 cells in our experimental setting, and, in line with this finding, blockade of $\alpha 4\beta 7$ integrin significantly affected Th17 trafficking, further suggesting a critical role for this adhesion molecule in Th17 migration and

leptomeningeal inflammation. It is known that in the absence of shear forces, such as those exerted during leukocyte extravasation, the induction of the high affinity state of integrins is not sufficient to support adhesive mechanisms during intratissue cell motility (77). Interestingly, it was previously demonstrated that, even in the absence of adhesive interactions, integrins are necessary for T cells locomotion mediating substrate friction between the actin cortex, controlled by chemokine receptors, and tissue environment (78), suggesting that this scenario may also verify during spinal SAS in EAE mice.

Previous studies have shown that $\alpha 4$ integrins are required for the maintenance of T cell “residency” in the CNS (79), suggesting this may be also the case for sustained permanence and pathological effects of Th17 cells in the meningeal space during EAE.

To further understand the relevance of Th17 $\alpha 4\beta 7$ integrin in meningeal inflammation and EAE development, we treated mice immunized with MOG₃₅₋₅₅ peptide (actively-induced EAE) by intrathecal administration of a blocking anti- $\alpha 4\beta 7$ integrin antibody. Notably, our results show that two doses of anti- $\alpha 4\beta 7$ antibody injected after disease onset were sufficient to significantly reduce disease severity and neuropathology, clearly substantiating the relevance of $\alpha 4\beta 7$ integrin in T cell locomotion and leptomeningeal inflammation. As expected, $\alpha 4\beta 7$ blockade also led to a reduction in CD3⁺ cell accumulation in the spinal cord without impacting T cells survival or activation, suggesting that therapeutic $\alpha 4\beta 7$ inhibition reduces T cell invasion. This underlines once more the importance of T cell motility inside the leptomeningeal structures in disease development. Moreover, even if we cannot exclude that *in vitro* differentiated Th cells rely on $\alpha 4\beta 7$ integrin more than endogenous ones, our intrathecal treatment approach, that resulted in a significant mitigation of EAE, further suggests our experimental approach as a reliable model of investigation. Intriguingly, the beneficial effect of anti- $\alpha 4\beta 7$ blockade on disease lasted for a long time, highlighting the pivotal role of Th17 cells in the maintenance of inflammatory responses during chronic disease progression.

In conclusion, our results show that $\alpha 4\beta 7$ integrin selectively controls Th17 cell adhesion in leptomeningeal vessels and trafficking inside the spinal cord SAS, potentially influencing subsequent parenchymal inflammation and contributing to vascular dysfunction and lesion distribution (80). Understanding the molecular mechanisms responsible for the specific contribution of Th1 and Th17 cells to the pathogenesis of autoimmune inflammatory disease of the CNS may help to identify new therapeutic strategies for these disorders.

Both EAE and neuromyelitis optica spectrum disorders (NMOSD) have been correlated to a preferential Th17 cells activity in optic nerves and spinal cord (81–83). However, although in both disorders Th17 migration into the spinal cord is considered a crucial pathogenic mechanism, natalizumab treatment in NMOSD patients proved ineffective (84), suggesting a more selective intervention on Th17 cells is needed. Also, the severe disease rebound showed by some RR-MS patients after long-term natalizumab treatment, is associated to a pathogenic profile in Th17 cells, including altered migratory features, further indicating that

therapies aimed at interfering with Th17 cell function may be beneficial in MS (85). Interestingly, *in vivo* systemic blockade of $\beta 7$ integrin subunit at disease peak during a transfer EAE model, induced a gradual disease remission. Moreover, when coinjected with anti- $\alpha 4$ antibody, this antibody potentiated the therapeutic effect of the anti- $\alpha 4$ treatment (73). Together, these data suggest that inhibition of $\alpha 4\beta 7$ integrin may have some beneficial effects over the anti- $\alpha 4$ therapy, especially in patients with high numbers of circulating Th17 cells and therefore, at elevated risk of disease rebound post natalizumab (86). Thus, in the context of existing literature, our results suggest that anti- $\alpha 4\beta 7$ antibodies, already in clinical use for subjects with inflammatory bowel diseases, may also be beneficial in patients with MS (87, 88).

Data availability statement

The original contributions presented in the study are included in the article/Supplementary Material. Further inquiries can be directed to the corresponding authors.

Ethics statement

The animal study was reviewed and approved by Institutional Animal Care Committee (OPBA) of the University of Verona.

Author contributions

BR, SD, GA, AB, NL, VD, EP, EZ, and CZ, performed the research. BR analyzed the data. BR and GC designed the study and wrote the paper. All authors contributed to the article and approved the submitted version.

Funding

This work was supported in part by the European Research Council grants: 261079 NEUROTRAFFICKING, 695714 IMMUNOALZHEIMER, 693606 IMPEDE and 101069397 NeutrAD (to GC), Fondazione Italiana Sclerosi Multipla (FISM), Genova, Italy (Cod. 2013/R/21 to BR), National Multiple Sclerosis Society (NMSS), New York, NY, USA (to GC), NEXTGENERATIONEU and Ministry of University and Research (MUR), National Recovery and Resilience Plan (PNRR), project MNESYS (PE0000006) (to GC). SD was supported by a fellowship from FISM (Cod. 2013/B/5).

Acknowledgments

We are grateful to Domenichini Nereo for assistance with EIVM and the Center for Technological Platforms (<https://cpt.univr.it>) from University of Verona for the TPLSM facility.

Conflict of interest

The authors declare that the research was conducted in the absence of any commercial or financial relationships that could be construed as a potential conflict of interest.

Publisher's note

All claims expressed in this article are solely those of the authors and do not necessarily represent those of their affiliated organizations, or those of the publisher, the editors and the reviewers. Any product that may be evaluated in this article, or claim that may be made by its manufacturer, is not guaranteed or endorsed by the publisher.

Supplementary material

The Supplementary Material for this article can be found online at: <https://www.frontiersin.org/articles/10.3389/fimmu.2023.1071553/full#supplementary-material>

SUPPLEMENTARY FIGURE 1

Characterization of *in vitro* polarized MOG₃₅₋₅₅-specific Th1 and Th17 cells. Th cell subpopulations were studied by flow cytometry to evaluate their cytokine production or adhesion molecules profile. (A) Representative gating strategy used to assess Th1 and Th17 cells for their specific patterns of cytokine production and trafficking receptors. (B) The percentages of IFN- γ +, IL-17+ and IFN- γ + IL-17+ Th1 (left panel) and Th17 (right panel) cells were evaluated by intracellular flow cytometry staining, as described in materials and methods. Data are expressed as mean \pm SEM from 12 independent experiments. (C) The percentages of Th1 (blue) and Th17 (red) cells expressing α 4 integrin, α 4 β 7 integrin, LFA-1 integrin, CD44, CD62L and PSGL-1 were assessed by flow cytometry after surface staining. Data are expressed as mean \pm SD from 12 independent productions of each Th cell subset. Statistics were calculated using two tailed Mann-Whitney test (* P = 0.0196; *** P = 0.0024). (D) Representative histograms plot and quantification of the MFI of α 4 integrin (upper left panel), α 4 β 7 integrin (upper central panel), LFA-1 integrin (upper right panel), CD44 (lower left panel), CD62L (lower central panel) and PSGL-1 (lower right panel) displayed by Th1 (blue) and Th17 cells (red). Data are expressed as mean \pm SD from 12 independent experiments of each Th cell subset. Statistics were calculated using two tailed Mann-Whitney test (* P < 0.05).

SUPPLEMENTARY FIGURE 2

α 4 β 7 integrin blockade does not affect Th1 cell rolling and arrest in the spinal cord pial vessels during preclinical EAE. *In vitro* differentiated Th1 cells were fluorescently labeled and intravenously injected into EAE recipient mice during the preclinical phase (9 dpi) of disease. EIVM imaging was conducted immediately after cell transfer. Rolling and arrest of Th1 cells were evaluated before and after anti- α 4 β 7 antibody treatment. One-way ANOVA followed by Dunnett's multiple comparison test were applied to compare the frequency of rolling and adhesion events after antibody treatment with control (considered 100%). Data are represented as mean \pm SEM from a minimum of 12 to a maximum of 24 venules from three independent experiments.

SUPPLEMENTARY TABLE I

Expression of adhesion molecules on Th1 and Th17 cells. Results are expressed as mean \pm SD of 24 independent *in vitro* productions (12 for Th1 cells and 12 for Th17 cells). MFI represents mean fluorescence intensity. Statistics were calculated using two tailed Mann-Whitney test.

SUPPLEMENTARY TABLE II

Diameter, hemodynamics, and rolling velocities of Th1 and Th17 cells in the SC at the different phases of EAE. The mean blood flow velocity (Vm), wall shear stress (WSS), and the percentage of rolling and arrested cells were calculated as described in Materials and Methods. At least 100 consecutive cells/venule were examined. The velocity of rolling cells was measured by digital frame-by-frame analysis of videotapes. Vroll are presented as median. Data are arithmetic mean \pm SD for hemodynamic parameters and mean \pm SEM for the percentages of rolling and arrest.

SUPPLEMENTARY TABLE III

Diameter, hemodynamics, and rolling velocities of Th1 cells treated with blocking antibodies. Vm, WSS, and the percentage of rolling and arrested cells were calculated as described in Materials and Methods. At least 100 consecutive cells/venule were examined. The velocity of rolling cells was measured by digital frame-by-frame analysis of videotapes. Rolling velocity (Vroll) are presented as median. Data are arithmetic mean \pm SD for hemodynamic parameters and mean \pm SEM for the percentages of rolling and arrest.

SUPPLEMENTARY TABLE IV

Diameter, hemodynamics, and rolling velocities of Th17 cells treated with blocking antibodies. Vm, WSS, and the percentage of rolling and arrested cells were calculated as described in Materials and Methods. At least 100 consecutive cells/venule were examined. The velocity of rolling cells was measured by digital frame-by-frame analysis of videotapes. Rolling velocity (Vroll) are presented as median. Data are arithmetic mean \pm SD for hemodynamic parameters and mean \pm SEM for the percentages of rolling and arrest.

SUPPLEMENTARY MOVIE 1

Representative movie obtained by EIVM of Th1 rolling (white edge) or firmly adhering (white asterisk) on spinal pial vessels in a MOG₃₅₋₅₅-immunized recipient mouse at disease peak. Th1 cells were intravenously injected immediately before the imaging. FITC-dextran was injected for vessel visualization and *in vitro* CMFDA-labeled Th1 cells were intravenously injected immediately before the imaging. Cells were manually analyzed frame by frame to determine the fraction of cells that were rolling or under firm adhesion on the total number of cells that entered that vessel. The fastest cell from 20 consecutive freely-flowing in each vessel was used to calculate hemodynamic parameters.

SUPPLEMENTARY MOVIE 2

Th1 cell dynamics in the spinal leptomeninges is not affected by anti- α 4 integrin local blockade. Representative videos of antigen specific Th1 cells tracking inside spinal cord SAS, before (left) and after (right) anti- α 4 integrins treatment in MOG₃₅₋₅₅-immunized mice at the peak of EAE. Th1 cell motility is not affected after local blockade, suggesting that locomotion of Th1 cells inside the spinal SAS during the disease peak is α 4-integrins independent. Vessels are visualized in green. Velocity barr = 0-0.2 μ m/s.

SUPPLEMENTARY MOVIE 3

Anti- α 4 integrin local blockade affected Th17 cell dynamics in the spinal leptomeninges. Representative videos of antigen specific Th17 cells tracking inside spinal cord SAS, before (left) and after (right) anti- α 4 integrins treatment in MOG₃₅₋₅₅-immunized mice at the peak of EAE. Th17 cell motility decreased after local blockade inside the spinal SAS during EAE peak, suggesting that Th17 cells locomotion is under α 4 integrins handle. Vessels are visualized in green. Velocity barr = 0-0.2 μ m/s.

SUPPLEMENTARY MOVIE 4

Local α 4 β 7 integrin blockade of MOG₃₅₋₅₅-specific Th17 cells significantly reduced their dynamics in the spinal cord SAS. Representative videos of antigen specific Th17 cells tracking inside spinal cord SAS, before (left) and after (right) anti- α 4 β 7 integrin treatment in MOG₃₅₋₅₅-immunized mice at the peak of EAE. Th17 cell motility is drastically reduced after local blockade, strongly indicating a critical role for α 4 β 7 integrin in the locomotion of Th17 cells inside the spinal SAS during the disease peak. Vessels are visualized in green. Velocity barr = 0-0.2 μ m/s.

References

- Ley K, Laudanna C, Cybulsky MI, Nourshargh S. Getting to the site of inflammation: the leukocyte adhesion cascade updated. *Nat Rev Immunol* (2007) 7(9):678–89. doi: 10.1038/nri2156
- Vestweber D. How leukocytes cross the vascular endothelium. *Nat Rev Immunol* (2015) 15(11):692–704. doi: 10.1038/nri3908
- Grayson MH, Hotchkiss RS, Karl IE, Holtzman MJ, Chaplin DD. Intravital microscopy comparing T lymphocyte trafficking to the spleen and the mesenteric lymph node. *Am J Physiol Heart Circ Physiol* (2003) 284(6):H2213–2226. doi: 10.1152/ajpheart.00999.2002
- Miller MJ, Wei SH, Cahalan MD, Parker I. Autonomous T cell trafficking examined *in vivo* with intravital two-photon microscopy. *Proc Natl Acad Sci U.S.A.* (2003) 100(5):2604–9. doi: 10.1073/pnas.2628040100
- Gelman AE, Li W, Richardson SB, Zinselmeyer BH, Lai J, Okazaki M, et al. Cutting edge: acute lung allograft rejection is independent of secondary lymphoid organs. *J Immunol* (2009) 182(7):3969–73. doi: 10.4049/jimmunol.0803514
- Li W, Nava RG, Bribrisco AC, Zinselmeyer BH, Spahn JH, Gelman AE, et al. Intravital 2-photon imaging of leukocyte trafficking in beating heart. *J Clin Invest* (2012) 122(7):2499–508. doi: 10.1172/JCI62970
- Natsuaki Y, Egawa G, Nakamizo S, Ono S, Hanakawa S, Okada T, et al. Perivascular leukocyte clusters are essential for efficient activation of effector T cells in the skin. *Nat Immunol* (2014) 15(11):1064–9. doi: 10.1038/ni.2992
- Bjelobaba I, Begovic-Kupresanin V, Pekovic S, Lavrnja I. Animal models of multiple sclerosis: focus on experimental autoimmune encephalomyelitis. *J Neurosci Res* (2018) 96(6):1021–42. doi: 10.1002/jnr.24224
- Reich DS, Lucchinetti CF, Calabresi PA. Multiple sclerosis. *N Engl J Med* (2018) 378(2):169–80. doi: 10.1056/NEJMr1401483
- Bartholomaeus I, Kawakami N, Odoardi F, Schlager C, Miljkovic D, Ellwart JW, et al. Effector T cell interactions with meningeal vascular structures in nascent autoimmune CNS lesions. *Nature* (2009) 462(7269):94–8. doi: 10.1038/nature08478
- Piccio L, Rossi B, Scarpini E, Laudanna C, Giagulli C, Issekutz AC, et al. Molecular mechanisms involved in lymphocyte recruitment in inflamed brain microvessels: critical roles for p-selectin glycoprotein ligand-1 and heterotrimeric (g)i-linked receptors. *J Immunol* (2002) 168(4):1940–9. doi: 10.4049/jimmunol.168.4.1940
- Constantin G. Chemokine signaling and integrin activation in lymphocyte migration into the inflamed brain. *J Neuroimmunol.* (2008) 198(1–2):20–6. doi: 10.1016/j.jneuroim.2008.04.023
- Fabene PF, Navarro Mora G, Martinello M, Rossi B, Merigo F, Ottoboni L, et al. A role for leukocyte-endothelial adhesion mechanisms in epilepsy. *Nat Med* (2008) 14(12):1377–83. doi: 10.1038/nm.1878
- Rossi B, Angiari S, Zenaro E, Budui SL, Constantin G. Vascular inflammation in central nervous system diseases: adhesion receptors controlling leukocyte-endothelial interactions. *J Leukoc Biol* (2011) 89(4):539–56. doi: 10.1189/jlb.0710432
- Zenaro E, Pietronigro E, Della Bianca V, Piacentino G, Marongiu L, Budui S, et al. Neutrophils promote alzheimer's disease-like pathology and cognitive decline via LFA-1 integrin. *Nat Med* (2015) 21(8):880–6. doi: 10.1038/nm.3913
- Pietronigro E, Zenaro E, Bianca VD, Dusi S, Terrabuio E, Iannoto G, et al. Blockade of alpha4 integrins reduces leukocyte-endothelial interactions in cerebral vessels and improves memory in a mouse model of alzheimer's disease. *Sci Rep* (2019) 9(1):12055. doi: 10.1038/s41598-019-48538-x
- Dusi S, Angiari S, Pietronigro EC, Lopez N, Angelini G, Zenaro E, et al. LFA-1 controls Th1 and Th17 motility behavior in the inflamed central nervous system. *Front Immunol* (2019) 10:2436. doi: 10.3389/fimmu.2019.02436
- Kunkl M, Frasca S, Amormino C, Volpe E, Tuosto L. T Helper cells: the modulators of inflammation in multiple sclerosis. *Cells* (2020) 9(2):482. doi: 10.3390/cells9020482
- Luster AD, Alon R, von Andrian UH. Immune cell migration in inflammation: present and future therapeutic targets. *Nat Immunol* (2005) 6(12):1182–90. doi: 10.1038/ni2175
- Bettelli E, Pagany M, Weiner HL, Linington C, Sobel RA, Kuchroo VK. Myelin oligodendrocyte glycoprotein-specific T cell receptor transgenic mice develop spontaneous autoimmune optic neuritis. *J Exp Med* (2003) 197(9):1073–81. doi: 10.1084/jem.20021603
- Rossi B, Zenaro E, Angiari S, Ottoboni L, Bach S, Piccio L, et al. Inverse agonism of cannabinoid CB1 receptor blocks the adhesion of encephalitogenic T cells in inflamed brain venules by a protein kinase α -dependent mechanism. *J Neuroimmunol.* (2011) 233(1–2):97–105. doi: 10.1016/j.jneuroim.2010.12.005
- Zenaro E, Rossi B, Angiari S, Constantin G. Use of imaging to study leukocyte trafficking in the central nervous system. *Immunol Cell Biol* (2013) 91(4):271–80. doi: 10.1038/icb.2012.81
- Kim JV, Kang SS, Dustin ML, McGavern DB. Myelomonocytic cell recruitment causes fatal CNS vascular injury during acute viral meningitis. *Nature* (2009) 457(7226):191–5. doi: 10.1038/nature07591
- Roth TL, Nayak D, Atanasiu T, Koretsky AP, Latour LL, McGavern DB. Transcranial amelioration of inflammation and cell death after brain injury. *Nature* (2014) 505(7482):223–8. doi: 10.1038/nature12808
- Herisson F, Frodermann V, Courties G, Rohde D, Sun Y, Vandoorne K, et al. Direct vascular channels connect skull bone marrow and the brain surface enabling myeloid cell migration. *Nat Neurosci* (2018) 21(9):1209–17. doi: 10.1038/s41593-018-0213-2
- Mazzitelli JA, Smyth LCD, Cross KA, Dykstra T, Sun J, Du S, et al. Cerebrospinal fluid regulates skull bone marrow niches *via* direct access through dural channels. *Nat Neurosci* (2022) 25(5):555–60. doi: 10.1038/s41593-022-01029-1
- Angiari S, Rossi B, Piccio L, Zinselmeyer BH, Budui S, Zenaro E, et al. Regulatory T cells suppress the late phase of the immune response in lymph nodes through p-selectin glycoprotein ligand-1. *J Immunol* (2013) 191(11):5489–500. doi: 10.4049/jimmunol.1301235
- Pardridge WM. CSF, blood-brain barrier, and brain drug delivery. *Expert Opin Drug Delivery* (2016) 13(7):963–75. doi: 10.1517/17425247.2016.1171315
- Butti E, Bergami A, Recchia A, Brambilla E, Del Carro U, Amadio S, et al. IL4 gene delivery to the CNS recruits regulatory T cells and induces clinical recovery in mouse models of multiple sclerosis. *Gene Ther* (2008) 15(7):504–15. doi: 10.1038/gt.2008.10
- McGavern DB, Murray PD, Rodriguez M. Quantitation of spinal cord demyelination, remyelination, atrophy, and axonal loss in a model of progressive neurologic injury. *J Neurosci Res* (1999) 58(4):492–504. doi: 10.1002/(sici)1097-4547(19991115)58:4<492::aid-jnr3>3.0.co;2-p
- Bishop JJ, Popel AS, Intaglietta M, Johnson PC. Rheological effects of red blood cell aggregation in the venous network: a review of recent studies. *Biorheology* (2001) 38(2–3):263–74.
- Makino A, Shin HY, Komai Y, Fukuda S, Coughlin M, Sugihara-Seki M, et al. Mechanotransduction in leukocyte activation: a review. *Biorheology* (2007) 44(4):221–49.
- Stroka KM, Aranda-Espinoza H. A biophysical view of the interplay between mechanical forces and signaling pathways during transendothelial cell migration. *FEBS J* (2010) 277(5):1145–58. doi: 10.1111/j.1742-4658.2009.07545.x
- Aranami T, Yamamura T. Th17 cells and autoimmune encephalomyelitis (EAE/MS). *Allergol. Int* (2008) 57(2):115–20. doi: 10.2332/allergolint.R-07-159
- Goverman J. Autoimmune T cell responses in the central nervous system. *Nat Rev Immunol* (2009) 9(6):393–407. doi: 10.1038/nri2550
- Kaskow BJ, Baecher-Allan C. Effector T cells in multiple sclerosis. *Cold Spring Harb Perspect Med* (2018) 8(4):a029025. doi: 10.1101/cshperspect.a029025
- Thompson AJ, Polman CH, Miller DH, McDonald WI, Brochet B, Filippi MMX, et al. Primary progressive multiple sclerosis. *Brain* (1997) 120(Pt 6):1085–96. doi: 10.1093/brain/120.6.1085
- Muller DM, Pender MP, Greer JM. A neuropathological analysis of experimental autoimmune encephalomyelitis with predominant brain stem and cerebellar involvement and differences between active and passive induction. *Acta Neuropathol* (2000) 100(2):174–82. doi: 10.1007/s004019900163
- Noseworthy JH, Lucchinetti C, Rodriguez M, Weinshenker BG. Multiple sclerosis. *N Engl J Med* (2000) 343(13):938–52. doi: 10.1056/NEJM200009283431307
- Simon JH. The contribution of spinal cord MRI to the diagnosis and differential diagnosis of multiple sclerosis. *J Neurol Sci* (2000) 172(Suppl 1):S32–35. doi: 10.1016/s0022-510x(99)00275-0
- Nociti V, Cianfoni A, Mirabella M, Caggiula M, Frisullo G, Patanella AK, et al. Clinical characteristics, course and prognosis of spinal multiple sclerosis. *Spinal Cord* (2005) 43(12):731–4. doi: 10.1038/sj.sc.3101798
- Stromnes IM, Cerretti LM, Liggitt D, Harris RA, Goverman JM. Differential regulation of central nervous system autoimmunity by T(H)1 and T(H)17 cells. *Nat Med* (2008) 14(3):337–42. doi: 10.1038/nm1715
- Axtell RC, de Jong BA, Boniface K, van der Voort LF, Bhat R, De Sarno P, et al. T Helper type 1 and 17 cells determine efficacy of interferon- β in multiple sclerosis and experimental encephalomyelitis. *Nat Med* (2010) 16(4):406–12. doi: 10.1038/nm.2110
- Popescu BF, Lucchinetti CF. Pathology of demyelinating diseases. *Annu Rev Pathol* (2012) 7:185–217. doi: 10.1146/annurev-pathol-011811-132443
- Axtell RC, Raman C, Steinman L. Type I interferons: beneficial in Th1 and detrimental in Th17 autoimmunity. *Clin Rev Allergy Immunol* (2013) 44(2):114–20. doi: 10.1007/s12016-011-8296-5
- Glatigny S, Duhon R, Oukka M, Bettelli E. Cutting edge: loss of alpha4 integrin expression differentially affects the homing of Th1 and Th17 cells. *J Immunol* (2011) 187(12):6176–9. doi: 10.4049/jimmunol.1102515
- Rothhammer V, Heink S, Petermann F, Srivastava R, Claussen MC, Hemmer B, et al. Th17 lymphocytes traffic to the central nervous system independently of alpha4 integrin expression during EAE. *J Exp Med* (2011) 208(12):2465–76. doi: 10.1084/jem.20110434
- Ley K, Kansas GS. Selectins in T-cell recruitment to non-lymphoid tissues and sites of inflammation. *Nat Rev Immunol* (2004) 4(5):325–35. doi: 10.1038/nri1351
- Chen J, Fujimoto C, Vistica BP, He J, Wawrousek EF, Kelsall B, et al. Active participation of antigen-nonspecific lymphoid cells in immune-mediated inflammation. *J Immunol* (2006) 177(5):3362–8. doi: 10.4049/jimmunol.177.5.3362

50. Kader M, Wang X, Piatak M, Lifson J, Roederer M, Veazey R, et al. Alpha4(+)-beta7(hi)CD4(+) memory T cells harbor most Th-17 cells and are preferentially infected during acute SIV infection. *Mucosal Immunol* (2009) 2(5):439–49. doi: 10.1038/mi.2009.90
51. Cox CA, Shi G, Yin H, Vistica BP, Wawrousek EF, Chan CC, et al. Both Th1 and Th17 are immunopathogenic but differ in other key biological activities. *J Immunol* (2008) 180(11):7414–22. doi: 10.4049/jimmunol.180.11.7414
52. O'Connor RA, Prendergast CT, Sabatos CA, Lau CW, Leech MD, Wraith DC, et al. Cutting edge: Th1 cells facilitate the entry of Th17 cells to the central nervous system during experimental autoimmune encephalomyelitis. *J Immunol* (2008) 181(6):3750–4. doi: 10.4049/jimmunol.181.6.3750
53. Kebir H, Kreymborg K, Ifergan I, Dodelet-Devillers A, Cayrol R, Bernard M, et al. Human TH17 lymphocytes promote blood-brain barrier disruption and central nervous system inflammation. *Nat Med* (2007) 13(10):1173–5. doi: 10.1038/nm1651
54. Murphy AC, Lalor SJ, Lynch MA, Mills KH. Infiltration of Th1 and Th17 cells and activation of microglia in the CNS during the course of experimental autoimmune encephalomyelitis. *Brain Behav Immun* (2010) 24(4):641–51. doi: 10.1016/j.bbi.2010.01.014
55. Lee YK, Turner H, Maynard CL, Oliver JR, Chen D, Elson CO, et al. Late developmental plasticity in the T helper 17 lineage. *Immunity* (2009) 30(1):92–107. doi: 10.1016/j.immuni.2008.11.005
56. Domingues HS, Mues M, Lassmann H, Wekerle H, Krishnamoorthy G. Functional and pathogenic differences of Th1 and Th17 cells in experimental autoimmune encephalomyelitis. *PLoS One* (2010) 5(11):e15531. doi: 10.1371/journal.pone.0015531
57. Geginat J, Paroni M, Maglie S, Alfen JS, Kastirr I, Gruarin P, et al. Plasticity of human CD4 T cell subsets. *Front Immunol* (2014) 5:630. doi: 10.3389/fimmu.2014.00630
58. Kivisakk P, Imitola J, Rasmussen S, Elyaman W, Zhu B, Ransohoff RM, et al. Localizing central nervous system immune surveillance: meningeal antigen-presenting cells activate T cells during experimental autoimmune encephalomyelitis. *Ann Neurol* (2009) 65(4):457–69. doi: 10.1002/ana.21379
59. Jordao MJC, Sankowski R, Brendecke SM, Sagar, Locatelli G, Tai YH, et al. Single-cell profiling identifies myeloid cell subsets with distinct fates during neuroinflammation. *Science* (2019) 363(6425):eaat7554. doi: 10.1126/science.aat7554
60. Mundt S, Mrdjen D, Utz SG, Greter M, Schreiner B, Becher B. Conventional DCs sample and present myelin antigens in the healthy CNS and allow parenchymal T cell entry to initiate neuroinflammation. *Sci Immunol* (2019) 4(31):eaau8380. doi: 10.1126/sciimmunol.aau8380
61. Sonar SA, Shaikh S, Joshi N, Atre AN, Lal G. IFN-gamma promotes transendothelial migration of CD4(+) T cells across the blood-brain barrier. *Immunol Cell Biol* (2017) 95(9):843–53. doi: 10.1038/icb.2017.56
62. Liu Y, Alahiri M, Ulloa B, Xie B, Sadiq SA. Adenosine A2A receptor agonist ameliorates EAE and correlates with Th1 cytokine-induced blood brain barrier dysfunction via suppression of MLCK signaling pathway. *Immun Inflammation Dis* (2018) 6(1):72–80. doi: 10.1002/iid3.187
63. Bonney S, Seitz S, Ryan CA, Jones KL, Clarke P, Tyler KL, et al. Gamma interferon alters junctional integrity via rho kinase, resulting in blood-brain barrier leakage in experimental viral encephalitis. *mBio* (2019) 10(4):e01675–19. doi: 10.1128/mBio.01675-19
64. Huppert J, Closhen D, Croxford A, White R, Kulig P, Pietrowski E, et al. Cellular mechanisms of IL-17-induced blood-brain barrier disruption. *FASEB J* (2010) 24(4):1023–34. doi: 10.1096/fj.09.141978
65. Saha A, Sarkar C, Singh SP, Zhang Z, Munasinghe J, Peng S, et al. The blood-brain barrier is disrupted in a mouse model of infantile neuronal ceroid lipofuscinosis: amelioration by resveratrol. *Hum Mol Genet* (2012) 21(10):2233–44. doi: 10.1093/hmg/dd3038
66. Setiadi AF, Abbas AR, Jeet S, Wong K, Bischof A, Peng J, et al. IL-17A is associated with the breakdown of the blood-brain barrier in relapsing-remitting multiple sclerosis. *J Neuroimmunol*. (2019) 332:147–54. doi: 10.1016/j.jneuroim.2019.04.011
67. Grabovsky V, Feigelson S, Chen C, Bleijs DA, Peled A, Cinamon G, et al. Subsecond induction of alpha4 integrin clustering by immobilized chemokines stimulates leukocyte tethering and rolling on endothelial vascular cell adhesion molecule 1 under flow conditions. *J Exp Med* (2000) 192(4):495–506. doi: 10.1084/jem.192.4.495
68. Berlin C, Berg EL, Briskin MJ, Andrew DP, Kilshaw PJ, Holzmann B, et al. Alpha 4 beta 7 integrin mediates lymphocyte binding to the mucosal vascular addressin MAdCAM-1. *Cell* (1993) 74(1):185–95. doi: 10.1016/0092-8674(93)90305-a
69. O'Neill JK, Butter C, Baker D, Gschmeissner SE, Kraal G, Butcher EC, et al. Expression of vascular addressins and ICAM-1 by endothelial cells in the spinal cord during chronic relapsing experimental allergic encephalomyelitis in the biozzi AB/H mouse. *Immunology* (1991) 72(4):520–5.
70. Kanwar JR, Kanwar RK, Wang D, Krissansen GW. Prevention of a chronic progressive form of experimental autoimmune encephalomyelitis by an antibody against mucosal addressin cell adhesion molecule-1, given early in the course of disease progression. *Immunol Cell Biol* (2000) 78(6):641–5. doi: 10.1046/j.1440-1711.2000.00947.x
71. Doring A, Pfeiffer F, Meier M, Dehouck B, Tauber S, Deutsch U, et al. TET inducible expression of the alpha4beta7-integrin ligand MAdCAM-1 on the blood-brain barrier does not influence the immunopathogenesis of experimental autoimmune encephalomyelitis. *Eur J Immunol* (2011) 41(3):813–21. doi: 10.1002/eji.201040912
72. Engelhardt B, Laschinger M, Schulz M, Samulowitz U, Vestweber D, Hoch G. The development of experimental autoimmune encephalomyelitis in the mouse requires alpha4-integrin but not alpha4beta7-integrin. *J Clin Invest* (1998) 102(12):2096–105. doi: 10.1172/JCI4271
73. Kanwar JR, Harrison JE, Wang D, Leung E, Mueller W, Wagner N, et al. Beta7 integrins contribute to demyelinating disease of the central nervous system. *J Neuroimmunol*. (2000) 103(2):146–52. doi: 10.1016/s0165-5728(99)00245-3
74. Ruegg C, Postigo AA, Sikorski EE, Butcher EC, Pytela R, Erle DJ. Role of integrin alpha 4 beta 7/alpha 4 beta p in lymphocyte adherence to fibronectin and VCAM-1 and in homotypic cell clustering. *J Cell Biol* (1992) 117(1):179–89. doi: 10.1083/jcb.117.1.179
75. Stuve O, Bennett JL. Pharmacological properties, toxicology and scientific rationale for the use of natalizumab (Tysabri) in inflammatory diseases. *CNS Drug Rev* (2007) 13(1):79–95. doi: 10.1111/j.1527-3458.2007.00003.x
76. Pesic M, Bartholomaeus I, Kyrtasous NI, Heissmeyer V, Wekerle H, Kawakami N. 2-photon imaging of phagocyte-mediated T cell activation in the CNS. *J Clin Invest* (2013) 123(3):1192–201. doi: 10.1172/JCI67233
77. Woolf E, Grigorova I, Sagiv A, Grabovsky V, Feigelson SW, Shulman Z, et al. Lymph node chemokines promote sustained T lymphocyte motility without triggering stable integrin adhesiveness in the absence of shear forces. *Nat Immunol* (2007) 8(10):1076–85. doi: 10.1038/ni1499
78. Hons M, Kopf A, Hauschild R, Leithner A, Gaertner F, Abe J, et al. Chemokines and integrins independently tune actin flow and substrate friction during intranodal migration of T cells. *Nat Immunol* (2018) 19(6):606–16. doi: 10.1038/s41590-018-0109-z
79. Graesser D, Mahooti S, Madri JA. Distinct roles for matrix metalloproteinase-2 and alpha4 integrin in autoimmune T cell extravasation and residency in brain parenchyma during experimental autoimmune encephalomyelitis. *J Neuroimmunol*. (2000) 109(2):121–31. doi: 10.1016/s0165-5728(00)00275-7
80. Gross CC, Schulte-Mecklenbeck A, Hanning U, Posevitz-Fejfar A, Korsukewitz C, Schwab N, et al. Distinct pattern of lesion distribution in multiple sclerosis is associated with different circulating T-helper and helper-like innate lymphoid cell subsets. *Mult Scler* (2017) 23(7):1025–30. doi: 10.1177/1352458516662726
81. Ishizu T, Oseogawa M, Mei FJ, Kikuchi H, Tanaka M, Takakura Y, et al. Intrathecal activation of the IL-17/IL-8 axis in opticospinal multiple sclerosis. *Brain* (2005) 128(Pt 5):988–1002. doi: 10.1093/brain/awh453
82. Li Y, Wang H, Long Y, Lu Z, Hu X. Increased memory Th17 cells in patients with neuromyelitis optica and multiple sclerosis. *J Neuroimmunol*. (2011) 234(1-2):155–60. doi: 10.1016/j.jneuroim.2011.03.009
83. Herges K, de Jong BA, Kolkowitz I, Dunn C, Mandelbaum G, Ko RM, et al. Protective effect of an elastase inhibitor in a neuromyelitis optica-like disease driven by a peptide of myelin oligodendroglial glycoprotein. *Mult Scler* (2012) 18(4):398–408. doi: 10.1177/1352458512440060
84. Kleiter I, Hellwig K, Berthele A, Kumpfel T, Linker RA, Hartung HP, et al. Failure of natalizumab to prevent relapses in neuromyelitis optica. *Arch Neurol* (2012) 69(2):239–45. doi: 10.1001/archneurol.2011.216
85. Janoschka C, Lindner M, Koppers N, Starost L, Liebmann M, Eschborn M, et al. Enhanced pathogenicity of Th17 cells due to natalizumab treatment: implications for MS disease rebound. *Proc Natl Acad Sci U.S.A.* (2023) 120(1):e2209944120. doi: 10.1073/pnas.2209944120
86. Haas J, Schneider K, Schwarz A, Korporal-Kuhnke M, Faller S, von Glehn F, et al. Th17 cells: a prognostic marker for MS rebound after natalizumab cessation? *Mult Scler* (2017) 23(1):114–8. doi: 10.1177/1352458516640609
87. Dubree NJ, Artis DR, Castaneda G, Marsters J, Sutherland D, Caris L, et al. Selective alpha4beta7 integrin antagonists and their potential as anti-inflammatory agents. *J Med Chem* (2002) 45(16):3451–7. doi: 10.1021/jm020033k
88. Zundler S, Becker E, Weidinger C, Siegmund B. Anti-adhesion therapies in inflammatory bowel disease-molecular and clinical aspects. *Front Immunol* (2017) 8:891. doi: 10.3389/fimmu.2017.00891